NASA Technical Memorandum 87317

IN-74-21

Summary of Investigations of Engine Response to Distorted Inlet Conditions

Thomas J. Biesiadny, Willis M. Braithwaite,
Ronald H. Soeder, and Mahmood Abdelwahab
Lewis Research Center
Cleveland, Ohio

Prepared for the
68th Meeting of the Propulsion and Energetics Panel
sponsored by AGARD
Munich, Germany, September 8-9, 1986

NASA

SUMMARY OF INVESTIGATIONS OF ENGINE RESPONSE TO DISTORTED INLET CONDITIONS

Thomas J. Biesiadny, Willis M. Braithwaite, Ronald H. Soeder,
and Mahmood Abdelwahab
National Aeronautics and Space Administration
Lewis Research Center
Cleveland, Ohio 44135 U.S.A.

E-3048

SUMMARY

A survey is presented of experimental and analytical experience of the NASA Lewis Research Center in engine response to inlet temperature and pressure distortions. There has been a continuing NASA effort over the past decade and a half to improve the understanding of the effects of inlet distortion on engine performance, particularly on the compression system performance. Results of experimental investigations and analytical modeling work at NASA are reviewed together with a description of the hardware and the techniques employed. Distortion devices successfully simulated inlet distortion, and knowledge was gained on compression system response to different types of distortion. A list of NASA research references is included.

INTRODUCTION

A persistent problem in the development of airbreathing propulsion systems for new aircraft, be they turbojet, turbofan or turboshaft engines, is the detrimental effect of nonuniform inlet flow on engine stability. When rotary-wing aircraft are operating near the ground (i.e., in ground effect), engine exhaust can be contained by the rotor downwash and recirculated to the engine inlet (Fig. 1, Ref. 1). With vertical/short takeoff and land (V/STOL) aircraft the jet stream impinges on the ground, flows outward from the impingement points, and eventually reaches the engine inlet. This leads to hot gas ingestion. Other potential sources of inlet flow distortion are gun- or rocket-exhaust gas ingestion, wakes from other aircraft, aircraft maneuvers, interaction of airframe and inlet, and off-design operation of the inlet.

The effect of this inlet distortion, be it a pressure or temperature distortion or a combination of the two, is that the power available is reduced along with the engine-compression-system surge margin (i.e., the difference between the operating line and surge line). The confident prediction of ingestion levels, or inlet distortion patterns, for any arbitrary aircraft/engine design and their effect on compression system performance requires a comprehensive set of design data not easily obtained. Ground-level engine tests and flight tests are required to measure the magnitude and the effects of inlet distortion on the engine in question.

A continuing experimental and analytical program has been in progress at the Lewis Research Center for more than a decade to further the understanding of inlet distortion and its effects on engine stability, particularly that of the compression system. This work includes investigations using turbojet, turbofan, and turboshaft engines subjected to distortions of inlet pressure, temperature, and a combination of pressure and temperature. As byproducts of these investigations, devices to generate steady-state and time-variant pressure and temperature distortions were developed.

The effects of inlet flow distortions as defined by total pressure variations were extensively investigated by NASA's predecessor, the National Advisory Committee for Aeronautics (NACA), in the 1950's. Relatively simple analytical models and indices were developed to predict the effects of pressure distortion on engine stability. However, in the 1960's, higher speed aircraft encountered stability problems not predicted by these models. It was determined that these problems were the result of time-varying inlet total pressure distributions. At that time it was deemed desirable to also investigate the effect of nonuniform inlet temperature on engine stability. Although temperature distortion caused several known aircraft incidents, it had not been examined except for a few investigations in the 1950's (Refs. 2 to 4).

In the mid-1960's NASA returned to the investigation of engine stability and inlet flow distortion. Prime interest was in time-variant pressure distortion and both steady-state and time-variant temperature distortions. The results of these investigations were incorporated into analytical models and thus provided a base for a better understanding of the phenomenon.

Steady-state and time-variant devices to create inlet temperature and pressure distortions, and combined temperature and pressure distortion were required to simulate the inlet flow distortion occurring in the field. NASA Lewis developed the devices which are described in this report. Highlights of results of the NASA work with these distortion devices over the past decade and a half are also presented.

Because of the large number of programs involving inlet distortion and its effects on engine performance, and the large amount of data generated in these programs, some limit to the information presented is required. This report reviews NASA investigations into the engine response to distorted inlet conditions and covers, briefly, the results of experimental investigations, some analytical modeling work, and hardware and techniques used to simulate inlet pressure and temperature distortions.

The presentation of experimental results is divided into three sections:

(1) Steady-state and time-variant temperature distortion
(2) Steady-state and time-variant inlet pressure distortion
(3) Steady-state combined inlet pressure and temperature distortion

Analytical modeling work and comparisons with experimental work are also presented. The devices used to create these distortions included screens, both stationary and rotatable, and a pressure jet system capable of injecting air counter to the inlet flow, thus canceling inlet air momentum, to create both dynamic and steady-state pressure distortions. Temperature distortions were created by using hydrogen-fueled temperature distortion generators of two different designs; the larger for experimental work involving turbojet and turbofan engines, and the smaller for turboshaft engine investigations.

TEMPERATURE DISTORTION

Temperature Distortion Generators

Gaseous hydrogen burners were used to develop inlet temperature distortion. Because of the larger flows required, the inlet temperature distortion tests involving turbojet and turbofan engines required a different temperature distortion generator design than that used for the turboshaft engine tests. In addition the power output shaft in the center of the turboshaft engine inlet ducting and bellmouth imposed different design requirements on the generator for that installation.

The gaseous hydrogen burner (Figs. 2 and 3) used for tests with the turbojet and turbofan engines was installed upstream of the inlet bellmouth (Ref. 5). Hydrogen was used because it is cleaner burning--generating water vapor rather than pollutants--and requires a lower fuel-to-air ratio for a given temperature rise than other fuels that were considered. Therefore, its effects on engine performance parameters are of much less concern. Also, the low flammability limits of hydrogen permitted low levels of temperature rise. In addition, flame propagation is faster than other fuels considered. This was borne out in early investigations, which showed that temperature rise rates of 10 000 K/sec could be generated (Fig. 4 and Ref. 6) and that the distortion pattern remained nearly constant as flow approached the engine inlet (Fig. 5 and Ref. 7). In Fig. 4 the indicated, or measured, temperatures were corrected for time lag, Mach number/pressure recovery, and radiation by using the procedures and equations found in Ref. 8. For the larger burners used with the turbofan and turbojet installations, the distance from the burner to the engine inlet was three to six duct diameters, while in the case of the generator for the turboshaft engine this distance was two duct diameters. A later version of the burner used for turbojet and turbofan testing (Fig. 6) has the capability of being remotely rotated $\pm 30°$ from the center position (Ref. 9). Each of the four quadrants, or circumferential extents, is individually controlled so that many combinations are possible. In addition, each gutter, or radial extent, in a quadrant is controllable. An added feature is that one quadrant is designed so that a 30° sector can be inserted if an extent smaller than 90° is desired. Rotating the burner distortion pattern past the engine instrumentation permits mapping of the distortion and its effect through the compressor by using minimal instrumentation.

There are additional features of the burners shown in Figs. 2, 3, and 6 which are worthy of note. Each quadrant of the burner has five swirl-can pilot burners. Also in each quadrant is an ignition source for the hydrogen, five annular flameholder gutters, one radial gutter, and tubes to supply the hydrogen to the proper location for ignition. The control system is capable of fast response for temperature transients by way of a high-speed valve. For the time-variant temperature distortions, the desired hydrogen pressure is established in a trapped volume upstream of the flow control valve and a high-speed valve for the specified quadrants (Fig. 7). The swirl-can pilot burners at those quadrants are lit, and the engine-inlet temperature distortion pattern is set prior to each transient. At each engine condition, circumferential extents of the fan inlet can be exposed to a range of peak temperature magnitudes and/or temperature rise rates. The rate and magnitude are functions of the pressure and quantity of trapped hydrogen, respectively. The pressure of the trapped hydrogen can be changed and the process repeated until a compressor stall limit is reached. For steady-state distortions the valves for the quadrants of interest are opened slowly until the desired temperature level is reached at the engine inlet.

The temperature distortion generator for turboshaft engine application can create both steady-state and time-variant temperature distortion at the engine inlet by using gaseous hydrogen. It is an adaptation of a device described in Ref. 10. The burner (Fig. 8) consists of eight individually controlled sectors, with three swirl-cup combustors (Fig. 9) per sector. These swirl cups for the turboshaft engine distortion generator are the same size as the swirl-can pilot burners used for the turbojet and turbofan engine temperature distortion generator. Many sector combinations, or temperature distortion patterns, were possible. The hydrogen distribution system from the fuel supply point to the swirl-cup combustors and its operation are described in detail in Ref. 11.

In a typical operation to find the response of the turboshaft engine to inlet temperature distortion, the swirl cups in those sectors where the temperature distortion was being imposed were lit (there were no pilots) while the engine was at idle. The hydrogen flow was adjusted, and the engine power was increased to the desired operating level. Once conditions were stabilized, the hydrogen flow was either increased to a fixed level to produce the desired steady-state distortion or, if a transient distortion

was desired, pulsed at increasingly greater pressures until stall occurred. Each pulse produced a unique combination of temperature rise and temperature rise rate at the engine inlet.

Temperature Distortion Results

The results of the temperature distortion investigations are categorized in terms of the effects of sensor location, distortion extent, distortion magnitude, and Reynolds number index (i.e., altitude operation) changes.

Inlet temperature distortion can have a significant effect on engine stability, especially when it causes the engine control to operate at an incorrect equivalent rotor speed (i.e., the equivalent speed under standard sea-level-static inlet conditions). When the inlet temperature sensor detects either the cold or hot part of the distorted flow, the control adjusts variable geometry accordingly and changes the compressor stall margin differently than if the sensor detects the warm average inlet temperature. Therefore the location of the sensor is critical to engine stability and to the analysis of temperature distortions.

As the extent of the distortion increased to a certain level, the engines tested were less tolerant of circumferential distortion at a fixed operating condition. Moreover, the results from an investigation involving steady-state temperature distortion and a turbojet engine revealed that between 90 and 180° extent there was no significant change in compression system response (Ref. 12). This was also true for time-variant distortion testing with a turboshaft engine, even though it had an integral inlet particle separator (Fig. 10 and Ref. 13). Figure 10 shows a leveling off of temperature rise with increasing extent as 180° is reached.

In general, diametrically opposed circumferential distortion sectors such as those shown in Fig. 11(a) have less effect on the compression system than single distorted sectors such as that shown in Fig. 11(b) (Ref. 12). While this was noted for a turbojet engine, it is also in agreement with results of temperature distortion experiments for the turboshaft engine with inlet particle separator (Fig. 12 and Ref. 13). The engine compression system was more tolerant not only of a balanced distortion such as 180° opposed distortion cells but also of such patterns as a four-per-revolution distortion uniformly spaced.

In addition to tests to determine the effect of circumferential distortion extent, the magnitude of the distortion and its effect on compressor performance were investigated. It was determined in Refs. 5 and 14 that, for the turbofan engine tested, the time-variant circumferential temperature distortion required to produce stall was independent of the rise rate (Fig. 13) and was a function of the equivalent steady-state distortion in the critical stage in the compressor. Thus the temperature distortion at the compressor face was greater than steady-state for increasing rise rates because of the time required for the flow (distortion) to reach the critical stage. In Fig. 13 it should be noted that below approximately 1000 K/sec the burner design did not permit high enough temperature rises for determining whether stall would occur at those conditions. However, since the steady-state threshold for stall was shown to be the same as that for the available time-variant data, it is assumed that the critical temperature rise is the same for the temperature rise rates between steady state and 1000 K/sec.

Attempts were made to measure the magnitude of the steady-state distortion required to surge the turboshaft engine. None of these attempts were successful because the distortion levels that could be imposed were limited by an engine-inlet hardware temperature limit. Another consideration was the engine-inlet particle separator. A simplified analysis of the compressor operating point of the turboshaft engine during these steady-state distortion tests indicated that the particle separator desensitized the engine to the extent of circumferential temperature distortion possibly by mixing the heated and unheated inlet air to produce a more uniform temperature profile at the compressor face.

Figure 14 shows a plot of the uniform-inlet-flow compressor map generated experimentally. It should be noted that the map was constructed by using inferred compressor inlet conditions because space limitations made it impossible for truly representative temperatures and pressures to be measured at that station. Plotted on the compressor map is a steady-state data point where a 180° circumferential temperature distortion was created at the particle separator inlet (solid triangle). The engine did not surge for these conditions up to the steady-state temperature limit for the engine inlet hardware. If it is assumed that the compressor inlet will see the 180° circumferential distortion imposed at the separator inlet, experience shows that the average compressor operating point will be on the normal operating line, as shown by the solid triangular symbol. This represents the compressor speed equated to standard sea-level-static conditions by using the average engine inlet temperature. From parallel-compressor-theory assumptions (Refs. 15 and 16), the two sectors of the compressor operate at the same pressure ratio but at different equivalent speeds, as indicated by the solid diamond symbol for the hot sector and the solid cone symbol for the cold sector. As shown, the hot-sector operating point is considerably to the left of the surge line, and the compressor should have surged. Since no surge occurred, it may be assumed that the compressor inlet did not see the pure 180° distortion pattern but probably saw a more homogeneous temperature leaving the particle separator.

Finally, with inlet temperature distortion present, it was also found that the Reynolds number index (RNI) affected the stall margin. As an example, for the turbojet,

even with a moderate distortion, the stall margin decreased as the RNI decreased from 0.65 to 0.30 (Fig. 15 and Ref. 12). However, this was not as pronounced as for the turbofan engine (Ref. 17).

PRESSURE DISTORTION

Pressure Distortion Generators

Steady-state pressure distortions were generated by two methods. The first, and older, method involved screens of different densities. The second method of generating steady-state and, in addition, time-variant distortions of the inlet total pressure used a NASA-developed air jet device (Refs. 18 and 19). The device and its position relative to the engine inlet, approximately one duct diameter upstream, are shown in Fig. 16. This device produces total pressure distortion patterns by the cancellation of inlet airflow momentum. This is accomplished by injection of secondary air into the inlet duct in the direction opposite to the primary flow. The device contains 54 individual jets divided into six 60° sectors of nine jets each. A remotely controlled, hydraulically driven valve governs the flow to each sector independently. The degree of pressure distortion is controlled by the amount of this flow.

Pressure Distortion Results

Discussion of the pressure distortion results includes highlights of the effects of both steady-state and time-variant distortions. These highlights include the effects of the distortion generator on inlet conditions, the effects of a total pressure distortion as it travels through the engine compression system, the effects of a distortion rotating with or opposed to engine rotation, the effects of the frequency of the distortion pattern, and the relation between steady-state and time-variant distortions.

The total pressure distortion did not change significantly when traveling from the source that produced it to the engine face (Fig. 17). The static pressure distortion, however, increased exponentially from the source to the leading edge of the compressor first-stage rotor blades (Fig. 18 and Refs. 20 and 21). The behavior of the static pressure distortion is the key to satisfying the inlet flow condition for the analytical model, as is explained in the section MODELING. For a single distortion zone in a constant-area duct, this static-pressure-distortion axial distribution can be represented by the following equation (Refs. 22 and 23):

$$\frac{DPS}{(DPS)IGV} = e^{(-x/R)}$$

where

DPS maximum - minimum static pressure at a location x

(DPS)IGV maximum - minimum static pressure at mean radius of IGV

IGV inlet guide vane assembly

x distance upstream of IGV

R mean radius of IGV

The rate at which the total pressure distortion is attenuated within the compressor increased with increasing rotor speed (Fig. 19 and Ref. 24). A total temperature distortion was generated by the two unequal pressure ratios created by the pressure distortion and was maximum at the exit. Since the compressor flow exits into a plenum (combustor), the static pressure is uniform. Also the exit Mach number is low, and therefore the total pressure distortion is small.

An inlet total pressure distortion rotating about the engine axis increased stall margin when the distortion pattern rotated in the opposite direction to the compressor rotation but decreased the stall margin when the distortion rotated in the same direction as the compressor rotation (see Fig. 20 and Ref. 25). The increase and decrease in stall margin are relative to the steady-state condition, where there is no rotation of the distortion. The decrease of stall margin is also a function of the rotational velocity of the distortion as a fraction of the rotor speed.

Other time-variant inlet total pressure distortions investigated were full-face-sinusoidal total pressure variations and 180° circumferential distortions, where (1) only the distorted sector, or the sector with its pressure below the average pressure, varied, and (2) both the distorted and undistorted sectors varied sinusoidally but 180° out of phase. As would be expected, the effect on the compressor was greater when both the distorted and undistorted sectors were active.

Discrete inlet pressure variations covering a variety of circumferential extents, amplitudes, and durations (or frequencies) for a given rotor speed were also investigated (Ref. 26). An example of this work is presented in Fig. 21, a plot of relative inlet total pressure amplitude as a function of pressure pulse duration, which shows the conditions that induced compressor stall for extents from 60 to 360°. Depending on the extent of the pressure distortion, this threshold was from a pulse duration of 5 to 14 msec, or a frequency of approximately 100 to 35 Hz, respectively. These data

indicate that stall is most likely to occur over a particular low frequency range, and the probability of it occurring above this range is low. A possible explanation for this behavior is that there is a finite time interval required for a rotor blade to stall in response to a total pressure distortion. During shorter durations, or higher frequencies, the distortion is too brief for a rotor blade to respond. The results showed that stall tolerance is a function of not only the instantaneous distortion level, but also the rate of change of the inlet pressure and the dwell-time of the fan-compressor rotor blading in an engine-inlet distortion.

It is possible to relate time-variant pressure distortions to steady-state distortions (Fig. 22) by using instantaneous distortion theory as presented in Ref. 27. Pressure distortions were observed with proper frequency filtering, or elimination of extraneous frequencies above and below the range of interest, or the critical frequency range. However, the effects of a given distortion pattern are a function of the particular geometry of an engine, such as combustor volume dynamics and compressor discharge conditions, and the results presented should only be used to show trends.

Overall it was found that a convenient descriptor for total pressure distortions was (max - min)/average. This can be related to individual and average compressor pressure ratios and their position on compressor maps.

COMBINED PRESSURE AND TEMPERATURE DISTORTION

Combined Pressure and Temperature Generators

To avoid undue complexity in analyzing the results, the study of combined temperature and pressure distortion was limited to a steady-state investigation of various combinations of 180° circumferential temperature and pressure patterns. The effect of combined pressure and temperature distortion on compressor stability limits was determined by slowly increasing the temperature in a 180° sector with a 180° extent distortion screen in place until stall was reached. Since the screen could be indexed independently of the temperature distortion generator, the effects of the relative positions of the pressure and temperature distortions could be investigated. A different approach was followed for the experimental investigation reported in Ref. 12. Stall data were obtained once an inlet distortion was established by reducing the exhaust nozzle area while maintaining constant equivalent engine speed.

Combined Pressure and Temperature Results

It was discovered that, when pressure and temperature patterns were fully overlapped, the distortion created in the compression system resulted in the greatest loss of stall margin (Refs. 21 and 28). If the combined pressure and temperature distortion were properly oriented, one distortion could counteract the other and actually increase stall margin. This occurred when there was no overlap of the distortions. Varying the amount of overlap resulted in a proportional loss in stall margin. Again, there was a minimum extent of combined distortion that reduced the stall margin.

By using the techniques involved in creating combined pressure and temperature distortion patterns, it was found that an operating envelope for an engine could be developed that defined the distortion sensitivity limits. For example, Soeder (Ref. 21) found that a distortion sensitivity map relating pressure and temperature distortion could be developed relatively easily by using a rotatable screen of approximately 50 percent density and a temperature distortion generator to cover both the full overlap and no overlap conditions for the pressure and temperature distortions (Fig. 23).

MODELING

An understanding of the effects of inlet flow distortions--pressure, temperature, and combined pressure and temperature--on stall margin can be obtained from a simplified model such as the one described in Refs. 15 and 16. These references also present a listing of some of the more common distortion indices and how they relate to the model. This theory predicted to a fair degree the pressure ratios and limiting distortions which cause compressor stall, but it did not consistently predict the equivalent air flow rates. However, the distorted and undistorted airflow rates were measured approximately 1 m in front of the engine inlet. Because static pressure distortion increases exponentially with distance along the inlet duct wall (Refs. 20 and 21), this discrepancy was reduced when the flows at the leading edge of the compressor first-stage blades were considered. Under NASA sponsorship this simplified model was further refined to yield a more reliable prediction for a low-bypass-ratio turbofan engine (Refs. 22 and 23).

NASA was also involved in other modeling efforts. These included the following: another low-bypass-ratio turbofan engine model (Ref. 29); a turbojet engine dynamic distortion model which provided a multipath analysis of circumferential temperature, pressure, and combined distortions (Refs. 30 and 31); and a high-bypass-ratio multispool engine compression system dynamic model (Ref. 32). However, to simplify this report only a representative sample (Refs. 22 and 23) of the modeling effort is presented. The steady-state model was more closely related to the experimental programs being conducted at NASA in addition to being a more well developed code before NASA's participation. Another consideration is that the models presented in Refs. 30 to 32 were dynamic models and as such were directed less toward inlet distortion and more toward stagnation stall, a subject beyond the scope of this report. Finally, the research emphasis at NASA has

shifted from inlet distortion, and therefore the dynamic models (Refs. 29 to 32) were not exercised extensively with experimental data.

An adaptation of the simplified model of Refs. 15 and 16, based on multiple flow paths (or parallel compressors) through the compression system, was developed by Mazzawy (Refs. 22 and 23) and extended under contract to achieve greater fidelity, especially with temperature distortion. Also, the model of the engine used for the experiment utilized compressor maps refined by using experimental data. Flows were permitted circumferentially across flow boundaries. Also, the temperature distortion was assumed to follow a particle through the compressor, whereas the pressure distortion was regarded as acoustic (Refs. 22 and 23) and exhibited less swirl in passing through the compressor. Comparison of the predictions obtained with this model and experimental data are presented in Ref. 28. This refined parallel compressor model was useful in obtaining an understanding of the stability phenomenon because it helped to relate pressure, temperature, and combined pressure and temperature distortions. A general list of the assumptions used in applying the refined parallel compressor theory are summarized as follows:

(1) The compressor is divided into subcompressor elements, with each element, or parallel compressor, operating as an identity defined by the undistorted compressor map.

(2) Swirl of the flow passing through the compressor is accounted for by the theory. The swirl associated with a pressure distortion is not identical to the swirl associated with a temperature distortion. Pressure passes through the compressor as an acoustic wave (i.e., little swirl), while temperature has the properties of a gas particle and follows the gas flow path (i.e., the temperature distortion has more swirl than the pressure distortion). This modifies the edges of the distortions, or blurs the distinction between distorted and undistorted regions.

(3) The exit static pressure is the same for all elements.

(4) For pressure distortion the elements operate at uniform equivalent rotor speed but at different pressure ratios dependent on the distortion, which results in unequal temperature ratios (i.e., pressure distortion is attenuated, and a temperature distortion is created).

(5) For temperature distortion, the elements operate at a constant pressure ratio, and therefore the temperature distortion is not modified except by inefficiency in the compressor.

(6) Individual element performance is adjusted to account for two-dimensional and unsteady flow effects, including engine-induced inlet flow redistribution, circumferential crossflows, and unsteady flow due to rotor movement through a distorted flow field.

In the work done by Braithwaite and Soeder (Ref. 28), it was reported that there was good agreement in duplicating analytically (Refs. 22 and 23) the experimental results by using the temperature and pressure profiles measured at the engine inlet. The flow angles measured at the engine inlet were satisfactorily duplicated analytically (Fig. 24). The internal response of the compression system, with regard to pressure and temperature profiles through the compressor (Fig. 25), swirl angles (Fig. 26), attenuation of the distortion (Fig. 27), and the values of limiting pressure and temperature distortions required to stall as determined analytically, was also found to be in good agreement with experimental results (Fig. 28).

The amount of pressure distortion required to stall the compression system is shown in Fig. 28 as a function of various levels of temperature distortion. Two regions are shown in the figure; one in which the high temperature is aligned with the low pressure region ($-\Delta T$), and one in which the high temperature and low pressure are opposed to each other (ΔT). For $-\Delta T$, or pure temperature distortion, it is shown that, as the temperature distortion decreases, larger total pressure distortions are required to stall the compression system until a pure pressure distortion is obtained. If the temperature distortion is then located in the opposite side of the inlet, increasing levels of pressure distortion are required for increasing temperature distortions. A second limit line is observed for the opposed distortions. For a pure temperature distortion, the distortion required to stall the engine is the same on either side of the engine. There is a stall region to the right of this point.

The refined parallel compressor model worked well when airflow was determined at the leading edge of the compressor first-stage blades, where high static pressure gradients exist. The experimental validation that static pressure distortion increases exponentially as the inlet flow approaches the compressor face (Refs. 20 and 21), previously mentioned in this section, was instrumental in explaining lack of agreement in equivalent inlet airflow rate between experimental data and the analytical model.

CONCLUDING REMARKS

A review of NASA Lewis experimental and analytical experience in engine response to inlet temperature and pressure distortions has been presented. Highlights of this work are the following:

1. Devices to generate inlet temperature and pressure distortion patterns have been developed and used successfully in conjunction with turbojet, turbofan, and turboshaft engines.

2. Inlet temperature distortion has a significant effect on engine stability.

3. The engines tested were less tolerant of circumferential temperature distortion at a fixed operating condition as the extent of the distortion increased.

4. Diametrically opposed temperature distortion sectors had less effect on the compression system than single distorted sectors.

5. A critical temperature distortion level, independent of temperature rise rate, had to be reached before stall occurred.

6. With inlet temperature distortion present, stall margin decreased as the Reynolds number index decreased.

7. The location of the engine-inlet temperature sensor can have a significant effect on response to inlet temperature distortion.

8. The total pressure and temperature distortions did not change significantly when traveling from the source that produced them to the engine inlet, but the static pressure distortion increased exponentially from the source to the engine inlet.

9. The compressor dissipated the total and static pressure distortions by the time the flow reached the compressor exit. However, a total temperature distortion was generated at the compressor exit.

10. A time-variant distortion pattern rotating in the opposite direction as the compressor rotation increased the stall margin, while a distortion rotating in the same direction decreased the stall margin relative to the steady-state condition. The decrease of stall margin is also a function of the rotational velocity of the distortion as a fraction of the rotor speed.

11. In general, stall could be achieved more easily at longer pulse durations which correspond to lower frequencies, but became more difficult as the duration decreased (i.e., higher frequencies) until a duration was reached where stall could not be achieved.

12. Combined pressure and temperature distortion patterns were used to generate a distortion sensitivity map which could be used as a guide to surge-free engine operation.

13. There was good agreement between experimental data and analytical models which were developed for the engines investigated. More work is required in this area before generalized models are available.

REFERENCES

1. Sheridan, P.F.; and Wiesner, W.: Aerodynamics of Helicopter Flight Near the Ground. AHS Paper 77-33-04, 1977.

2. Wallner, L.E.; Useller, J. W.; and Saari, M. J.: A Study of Temperature Transients at the Inlet of a Turbojet Engine. NACA RM-E57C22, 1957.

3. Gabriel, D.; Wallner, L.; Lubick, R.; and Vasu, G.: Some Effects of Inlet Pressure and Temperature Transients on Turbojet Engines. Aeronaut. Eng. Rev., vol. 16, no. 9, Sept. 1957, pp. 54-59, 68.

4. Childs, J.H.; et al.: Stall and Flame-Out Resulting from Firing of Armament. NACA RM-E55E25, 1955.

5. Braithwaite, W.M.: Experimental Evaluation of a TF30-P-3 Turbofan Engine in an Altitude Facility: Effect of Steady-State Temperature Distortion. NASA TM X-2921, 1973.

6. Rudey, R.A.; and Antl, R.J.: The Effect of Inlet Temperature Distortion on the Performance of a Turbofan Engine Compressor System. AIAA Paper 70-625, June 1970.

7. Soeder, R.H.; and Bobula, G.A.: Effect of Steady-State Temperature Distortion and Combined Distortion on Inlet Flow to a Turbofan Engine. NASA TM-79237, 1979.

8. Glawe, G.E.; Simmons, F.S.; and Stickney, T.M.: Radiation and Recovery Corrections and Time Constants of Several Chromel-Alumel Thermocouple Probes in High-Temperature, High-Velocity Gas Streams. NACA TN-3766, 1956.

9. Abdelwahab, Mahmood: Effects of Fan Inlet Temperature Disturbances on the Stability of a Turbofan Engine. NASA TM-82699, 1981.

10. Pawlik, E.V.; and Jones, R.E.: Experimental Evaluation of Swirl-Can Elements for Propane-Fuel Combustor. NASA Memo 5-15-59E, 1959.

11. Klann, G.A.; Barth, R.L.; and Biesiadny, T.J.: Temperature Distortion Generator for Turboshaft Engine Testing. Advances in Aerospace Propulsion, SAE SP-594, SAE, 1984, pp. 89-99.

12. Mehalic, C.M.; and Lottig, R.A.: Steady-State Inlet Temperature Distortion Effects on the Stall Limits of a J85-GE-13 Turbojet Engine. NASA TM X-2990, 1974.

13. Biesiadny, T.J.; Klann, G.A.; and Little, J.K.: Response of a Small-Turboshaft-Engine Compression System to Inlet Temperature Distortion. NASA TM-83765, 1984.

14. Abdelwahab, Mahmood: Effects of Temperature Transients at Fan Inlet of a Turbofan Engine. NASA TP-1031, 1977.

15. Graber, E.J.; and Braithwaite, W.M.: Summary of Recent Investigations of Inlet Flow Distortion Effects on Engine Stability. AIAA Paper 74-236, Jan. 1974.

16. Braithwaite, W.M.; Graber, E.J, Jr.; and Mehalic, C.M.: The Effect of Inlet Temperature and Pressure Distortion on Turbojet Performance. AIAA Paper 73-1316, Nov. 1973.

17. Soeder, R.H.; Mehalic, C.M.; and Stancik, K.: Effect of Steady-State Temperature Distortion on Inlet Flow to a High-Bypass-Ratio Turbofan Engine. NASA TM-86896, 1985.

18. Meyer, C.L.; McAulay, J.E.; and Biesiadny, T.J.: Technique for Inducing Controlled Steady-State and Dynamic Inlet Pressure Disturbances for Jet Engine Tests. NASA TM X-1946, 1970.

19. Baumbick, R.J.: Device for Producing Dynamic Distortion Patterns at Inlets of Air-Breathing Engines. NASA TM X-2026, 1970.

20. Soeder, R.H.; and Bobula, G.A.: Effect of Steady-State Pressure Distortion on Flow Characteristics Entering a Turbofan Engine. NASA TM-79134, 1979.

21. Soeder, R.H.; and Mehalic, C.M.: Effect of Combined Pressure and Temperature Distortion Orientation on High-Bypass-Ratio Turbofan Engine Stability. NASA TM-83771, 1984.

22. Mazzawy, R.S.; and Banks, G.A.: Modeling and Analysis of the TF30-P-3 Compressor System with Inlet Pressure Distortion. (PWA-5302, Pratt and Whitney Aircraft; NASA Contract NAS3-18535.) NASA CR-134996, 1976.

23. Mazzawy, R.S.; and Banks, G.A.: Circumferential Distortion Modeling of the TF30-P-3 Compression System. (PWA-5448, Pratt and Whitney Aircraft; NASA Contract NAS3-18535.) NASA CR-135124, 1977.

24. deBogdan, C.E.; et al.: Effect of a 180°-Extent Inlet Pressure Distortion on the Internal Flow Conditions of a TF30-P-3 Engine. NASA TM X-3267, 1975.

25. McAulay, J.E.: Effect of Dynamic Variations in Engine-Inlet Pressure on the Compressor System of a Twin-Spool Turbofan Engine. NASA TM X-2081, 1970.

26. Wenzel, L.M.: Experimental Investigation of the Effects of Pulse Pressure Distortions Imposed on the Inlet of a Turbofan Engine. NASA TM X-1928, 1969.

27. Melick, H.C.; and Simkin, W.E.: A Unified Theory of Inlet/Engine Compatibility. AIAA Paper 72-1115, Nov. 1972.

28. Braithwaite, W.M.; and Soeder, R.H.: Combined Pressure and Temperature Distortion Effects on Internal Flow of a Turbofan Engine. AIAA Paper 79-1309, June 1979.

29. Mazzawy, R.S.; Fulkerson, D.A.; Haddad, D.E.; and Clark, T.A.: F100(3) Parallel Compressor Computer Code and User's Manual Final Report. (PWA-5549-8, Pratt and Whitney Aircraft; NASA Contract NAS3-20610.) NASA CR-135388, 1978.

30. Tesch, W.A.; and Steenken, W.G.: Blade Row Dynamic Digital Compressor Program, Volume I, J85 Clean Inlet Flow and Parallel Compressor Models. (R75-AEG406, General Electric; NASA Contract NAS3-18526.) NASA CR-134978, 1976.

31. Tesch, W.A.; and Steenken, W.G.: Blade Row Dynamic Digital Compressor Program, Volume II, J85 Circumferential Distortion Redistribution Model, Effect of Stator Characteristics, and Stage Characteristics Sensitivity Study. (R76-AEG484-VOL-2, General Electric; NASA Contract NAS3-18526.) NASA CR-134953, 1978.

32. Hosny, W.M.; and Steenken, W.G.: TF34 Engine Compression System Computer Study. (R78-AEG612, General Electric; NASA Contract NAS3-20599.) NASA CR-159889, 1979.

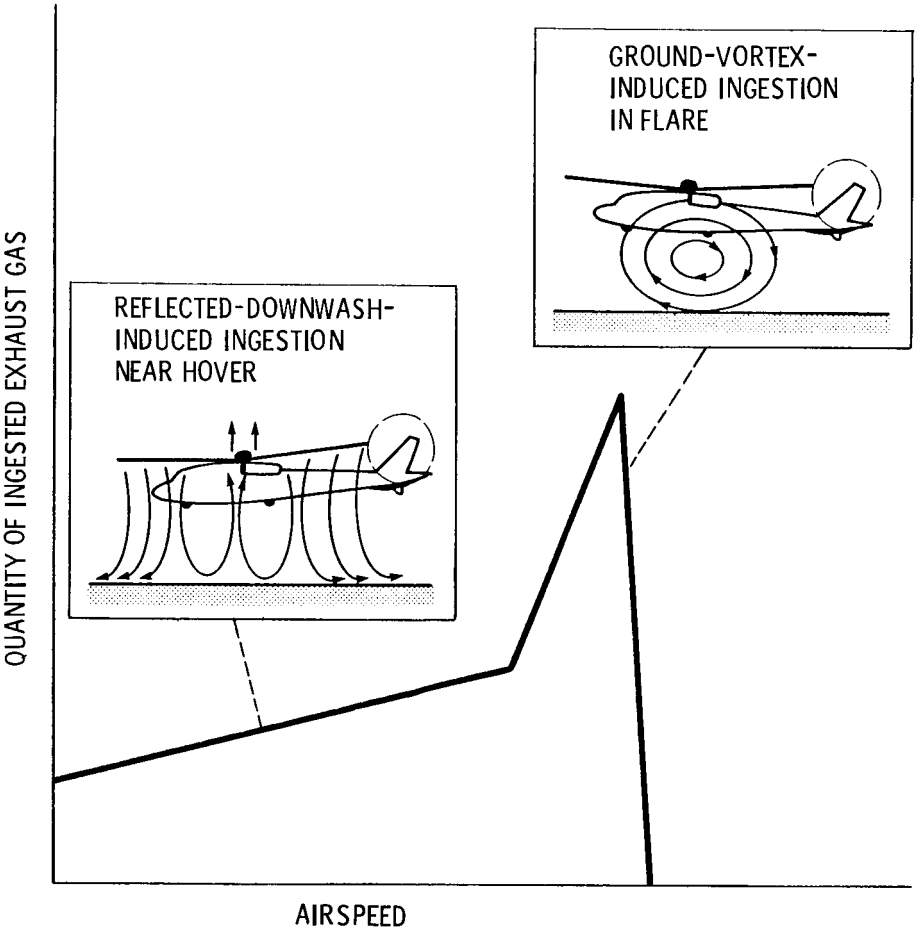

Figure 1. - Patterns of exhaust ingestions near ground (from ref. 1).

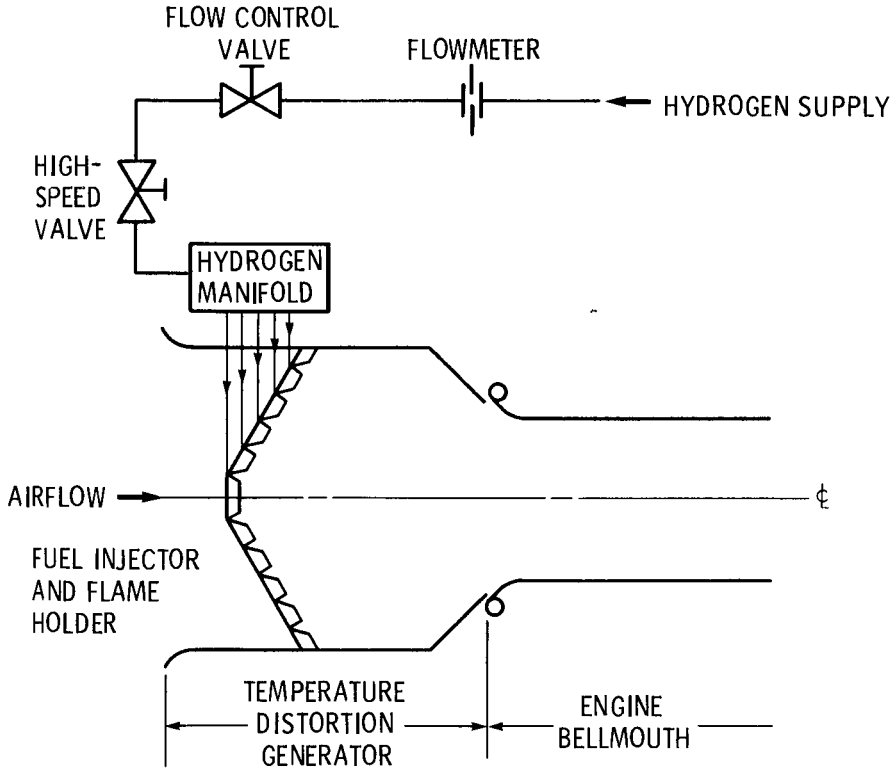

Figure 2. - Hydrogen-fueled temperature distortion generator.

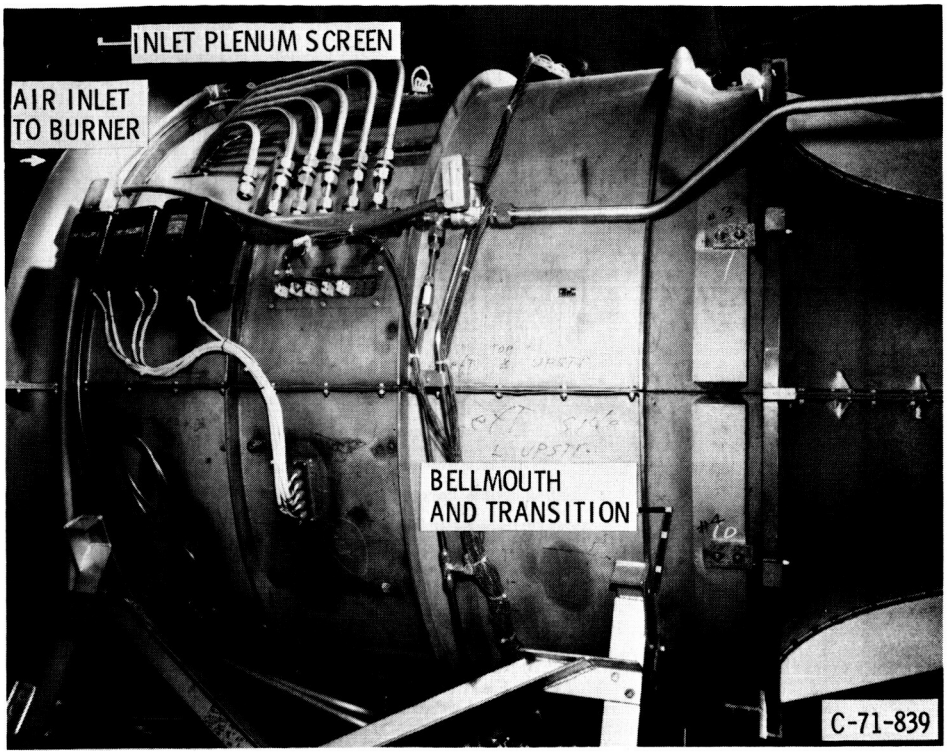

(a) External view.

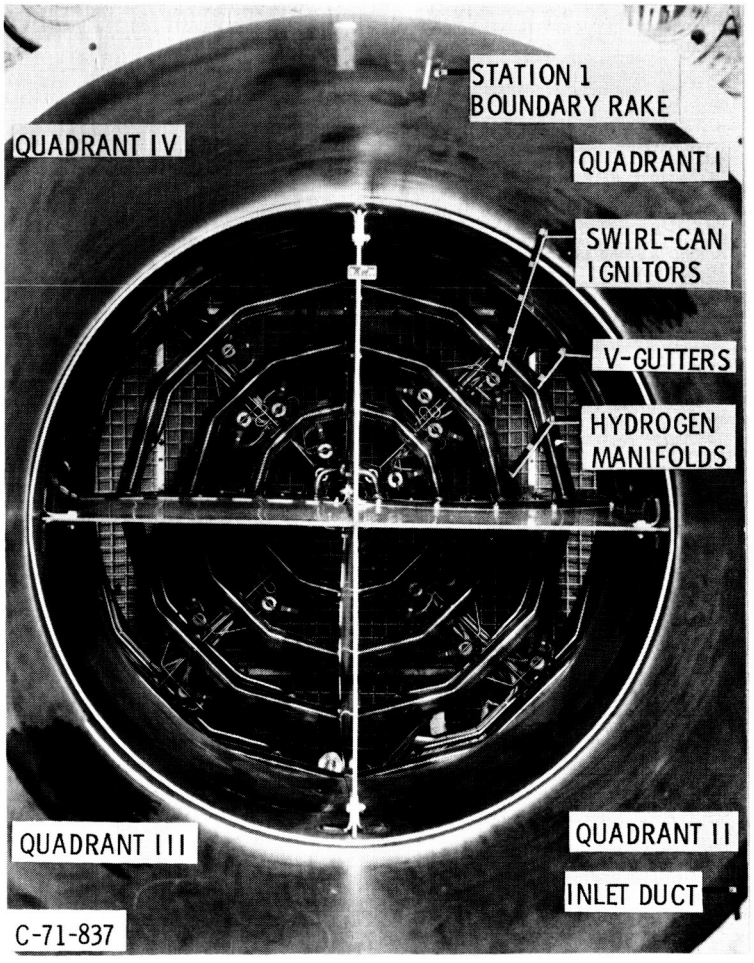

(b) Internal view looking forward.

Figure 3. - Gaseous hydrogen burner installed in altitude chamber.

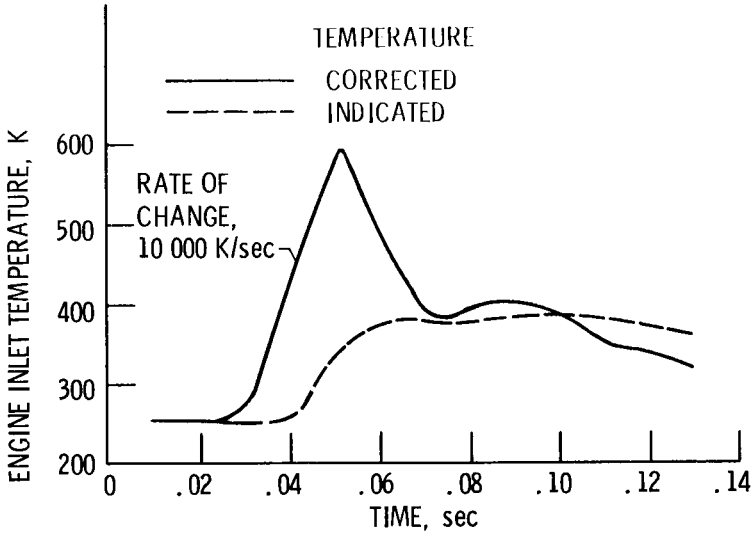

Figure 4. - Typical engine inlet temperature transients.

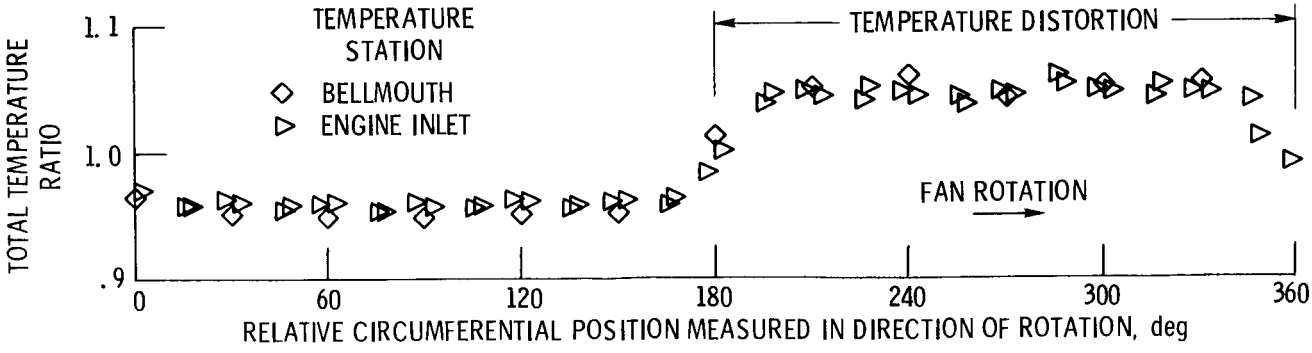

Figure 5. - Circumferential variation of total temperature profiles.

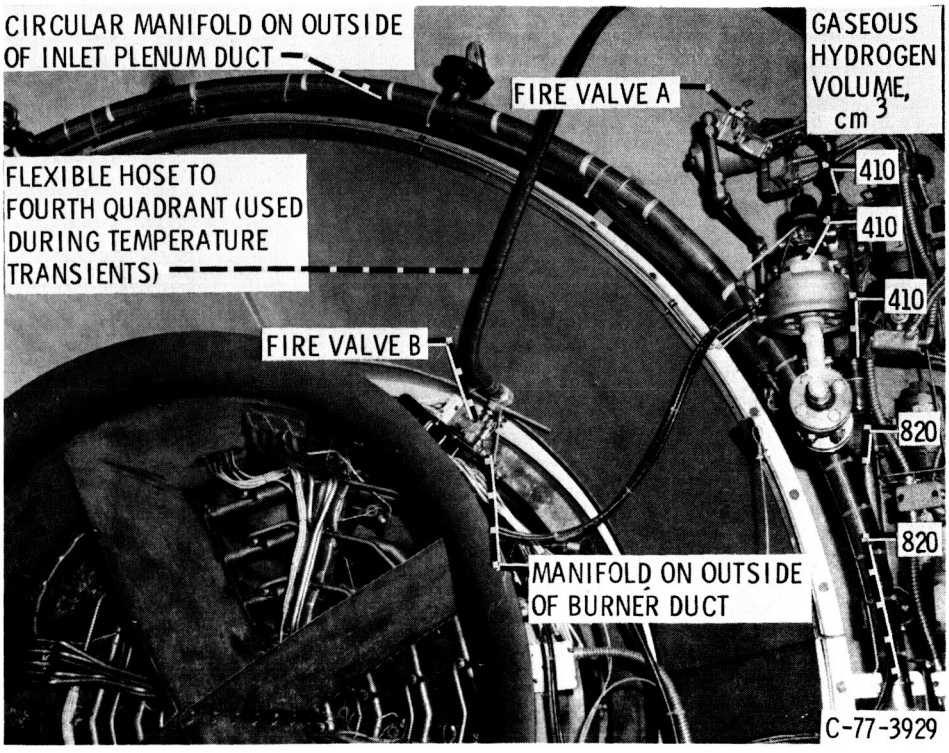

(a) For producing temperature transients.

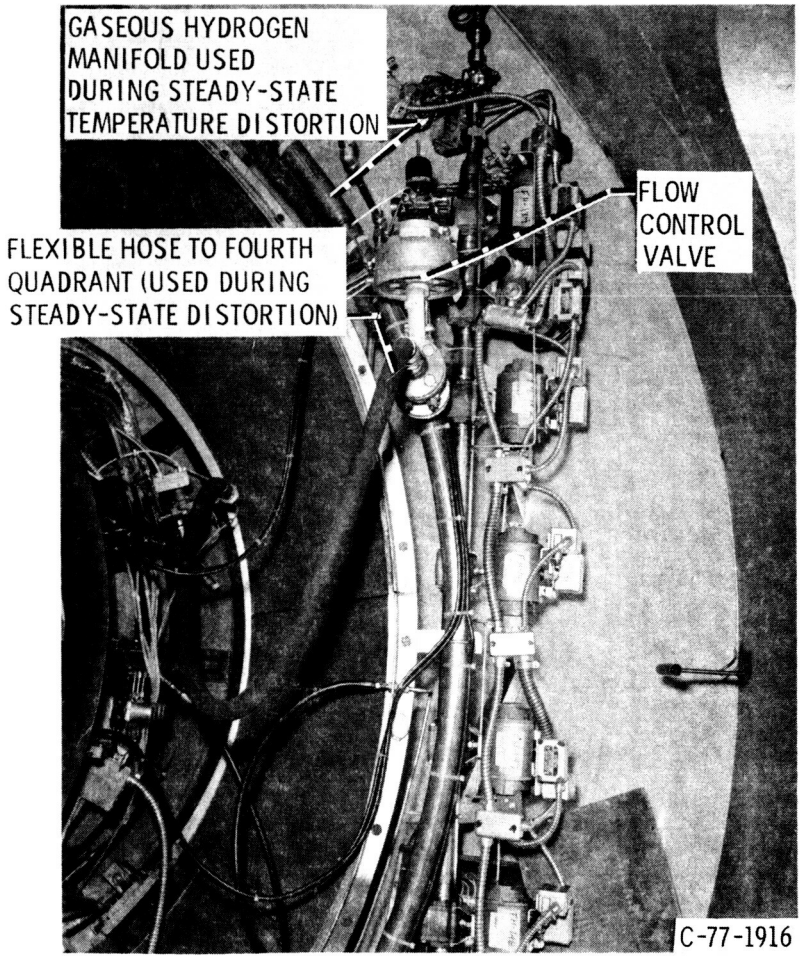

(b) For producing steady-state distortion.

Figure 6. - Gaseous-hydrogen-fueled burner (quadrant IV) installation.

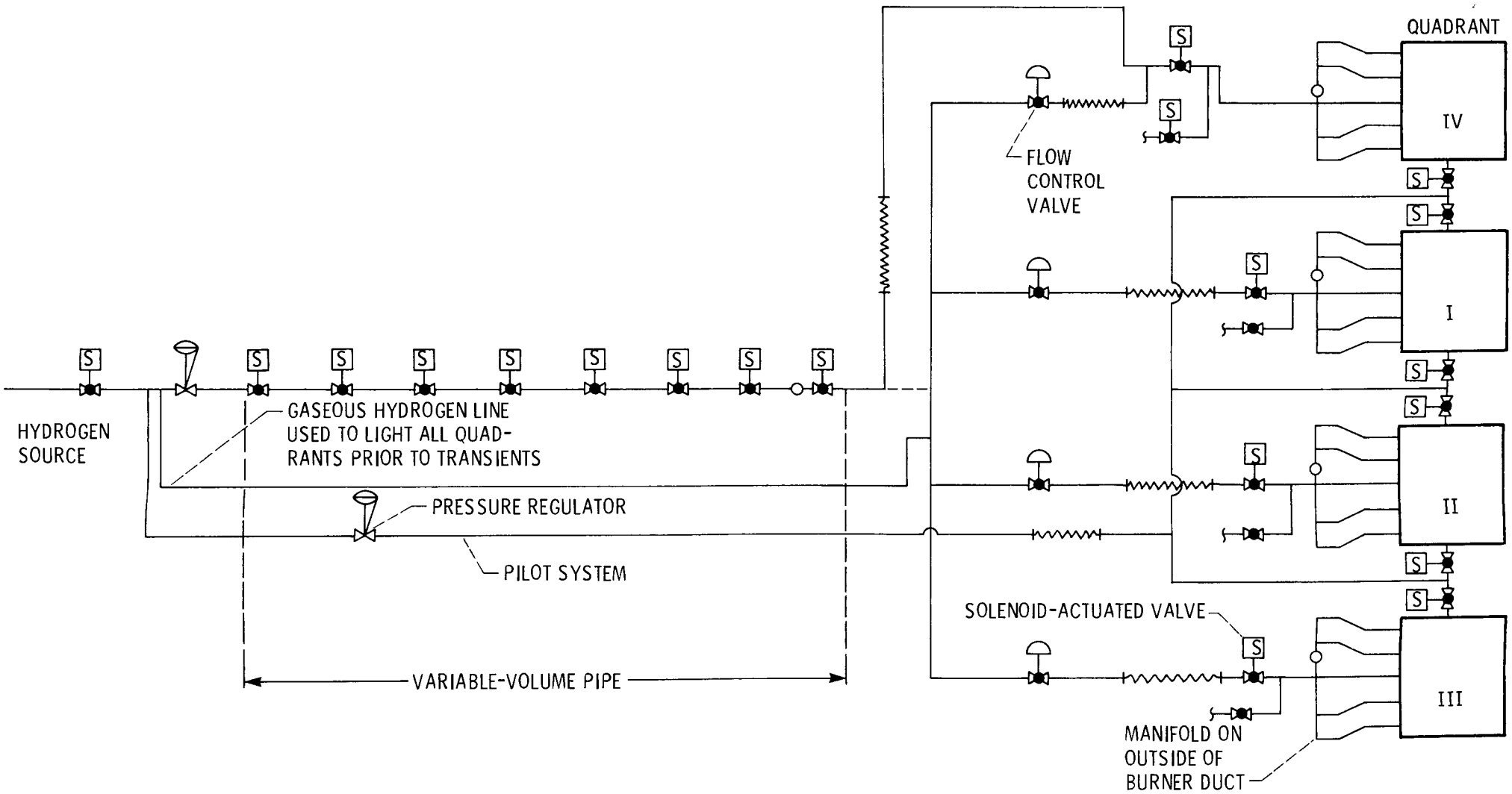

Figure 7. - Gaseous-hydrogen-fueled burner schematic.

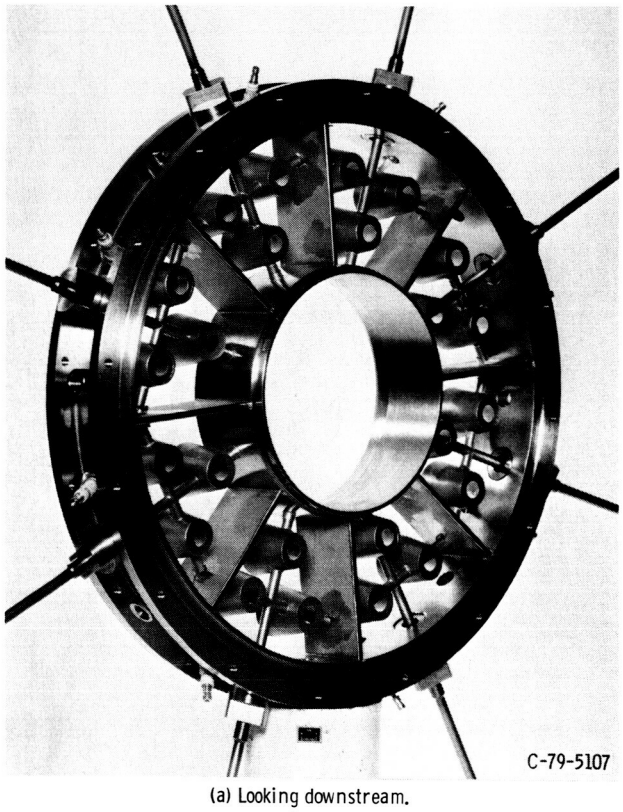

(a) Looking downstream.

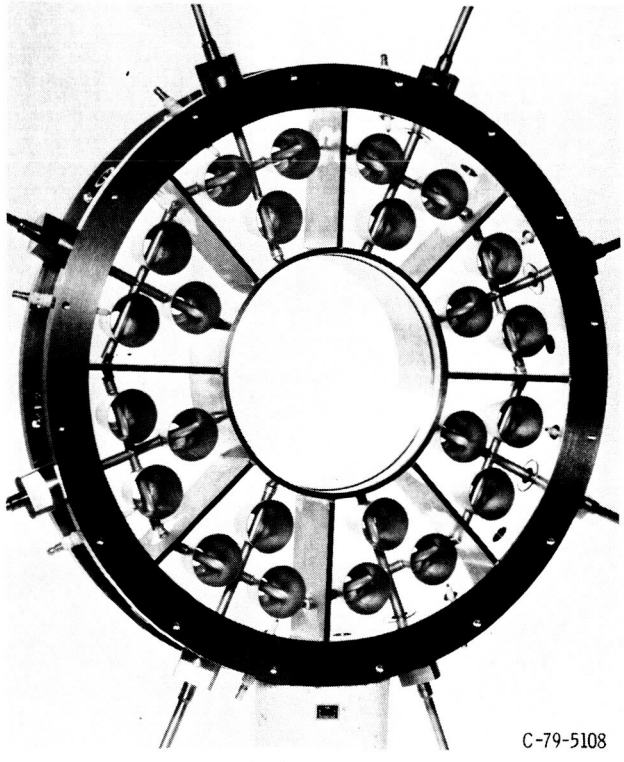

(b) Looking upstream.

Figure 8. - Temperature distortion generator for turboshaft engine testing.

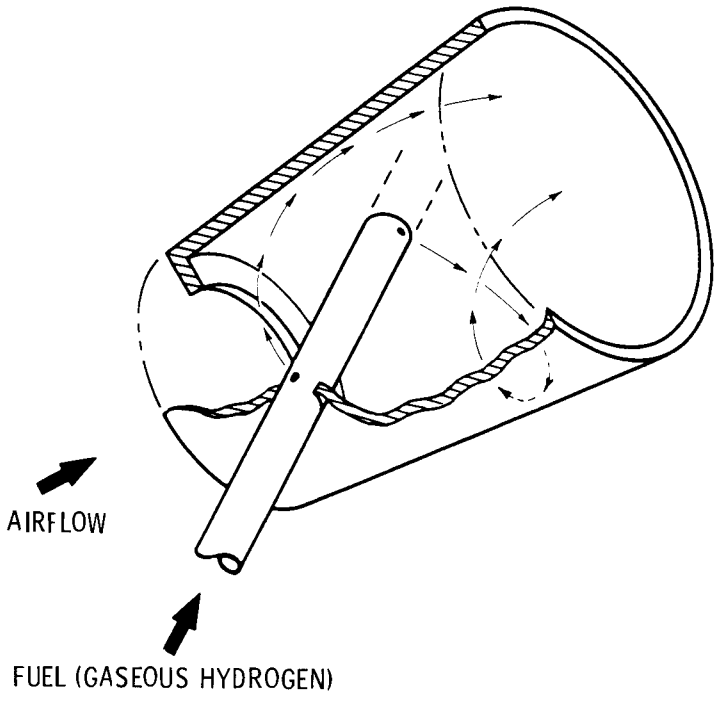

Figure 9. - Operation of typical swirl-cup combustor.

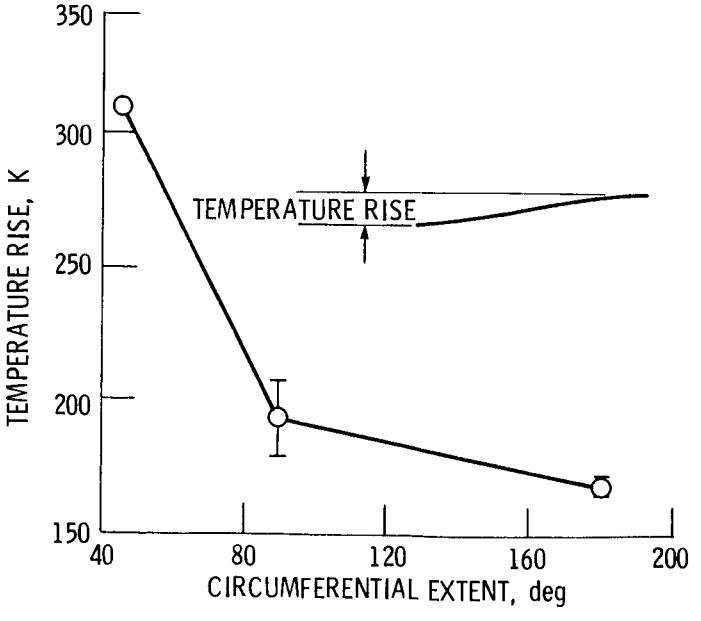

Figure 10. - Inlet temperature rise before onset of surge as a function of circumferential extent.

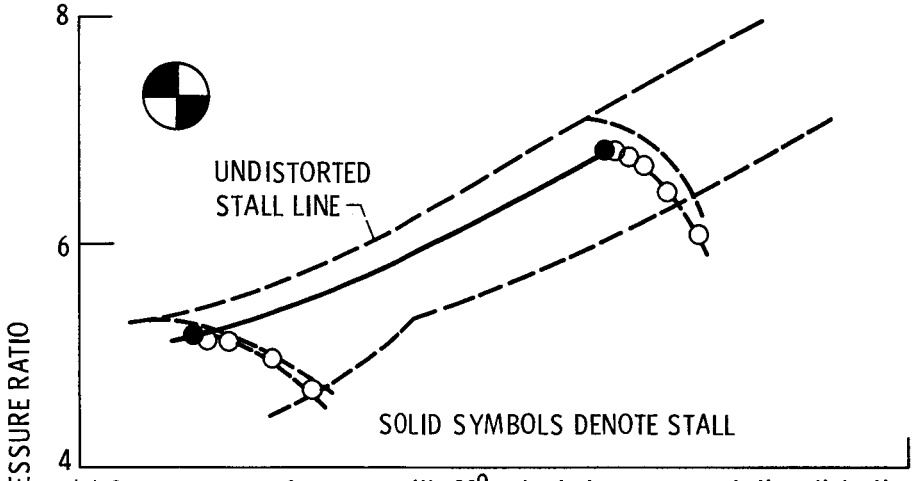

(a) Compressor performance with 90^0 extent, two-per-revolution distortion.

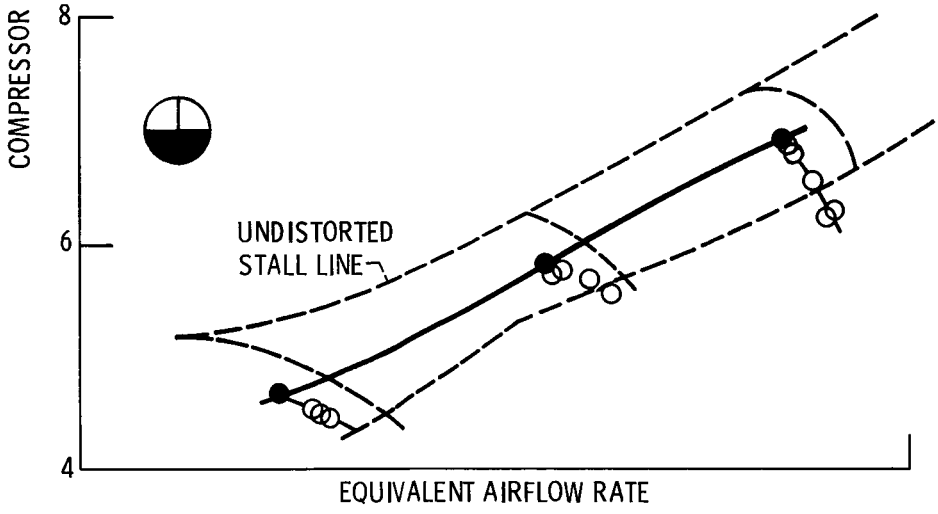

(b) Compressor performance with 180^0 extent circumferential distortion.

Figure 11. - Comparison of single distorted zone and diametrically opposed distorted zones.

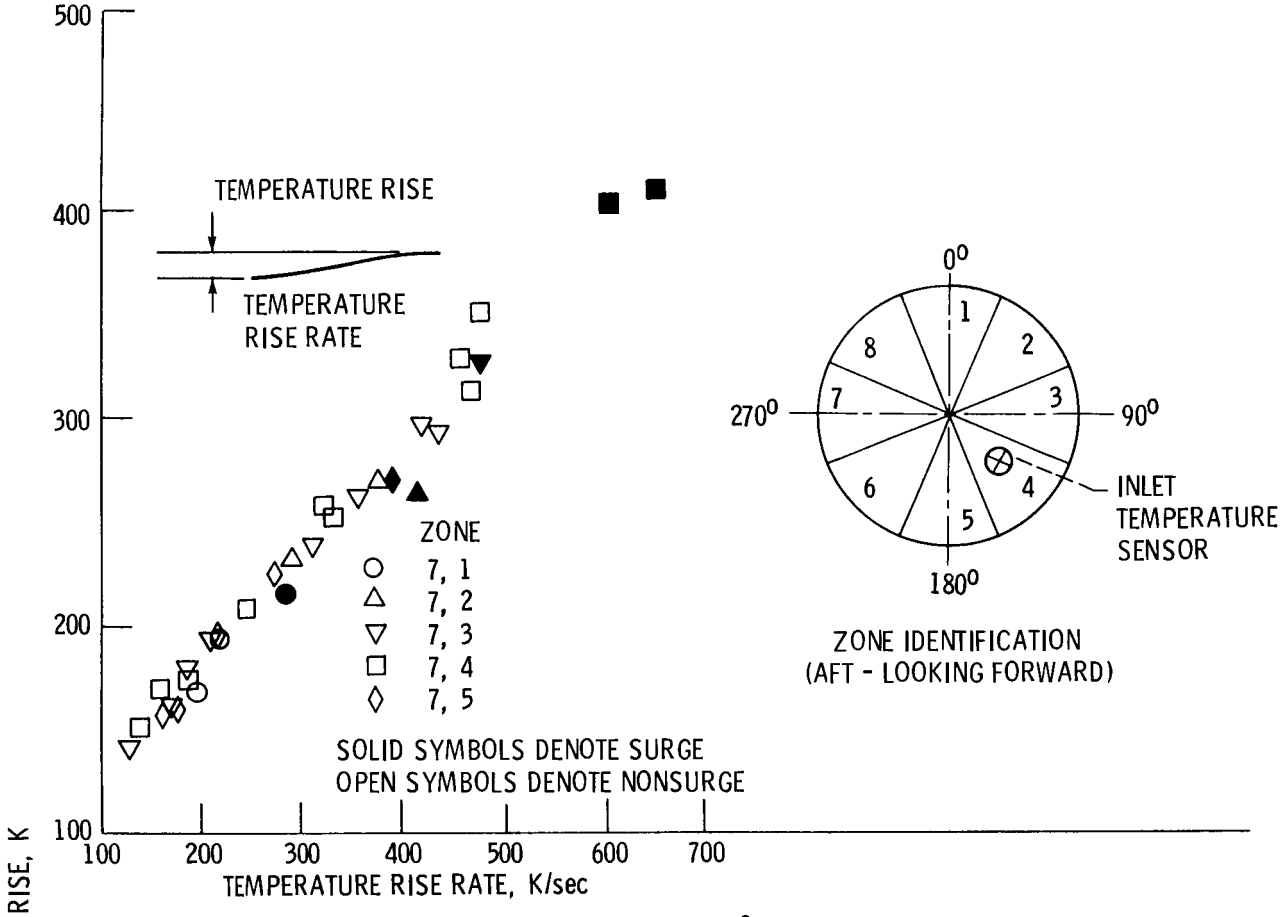

(a) Two nonadjacent 45° extents.

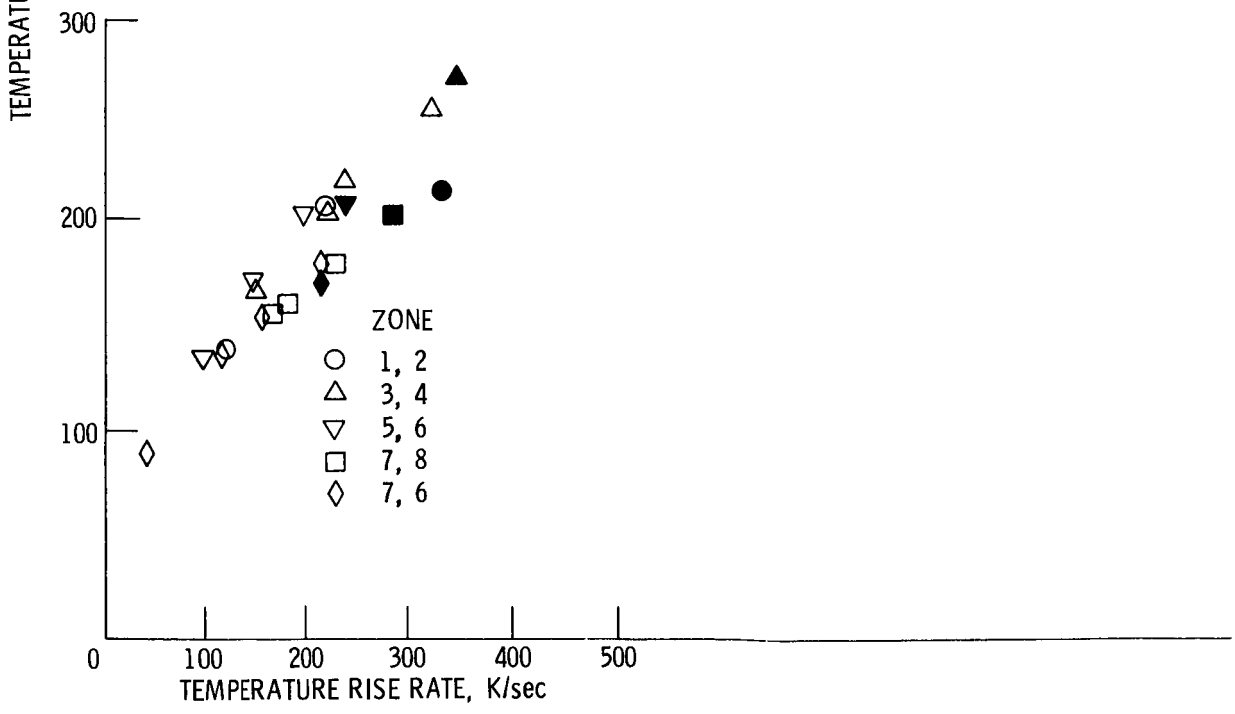

(b) Two adjacent 45° extents.

Figure 12. - Comparison of adjacent and nonadjacent distorted zones for a turboshaft engine.

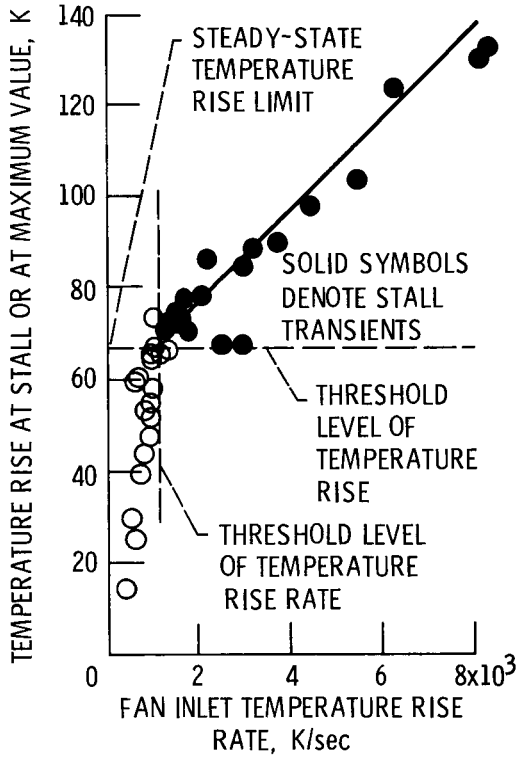

Figure 13. - Fan inlet temperature rise as a function of temperature rise rate.

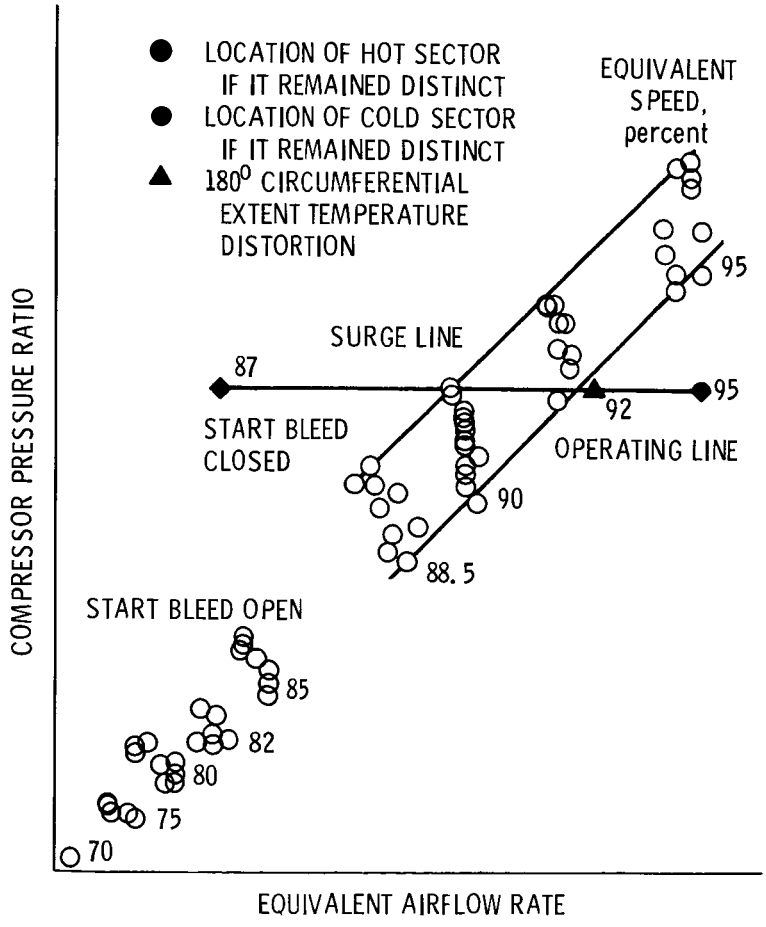

Figure 14. - Typical compressor performance map, showing effects of mixed and unmixed distorted areas.

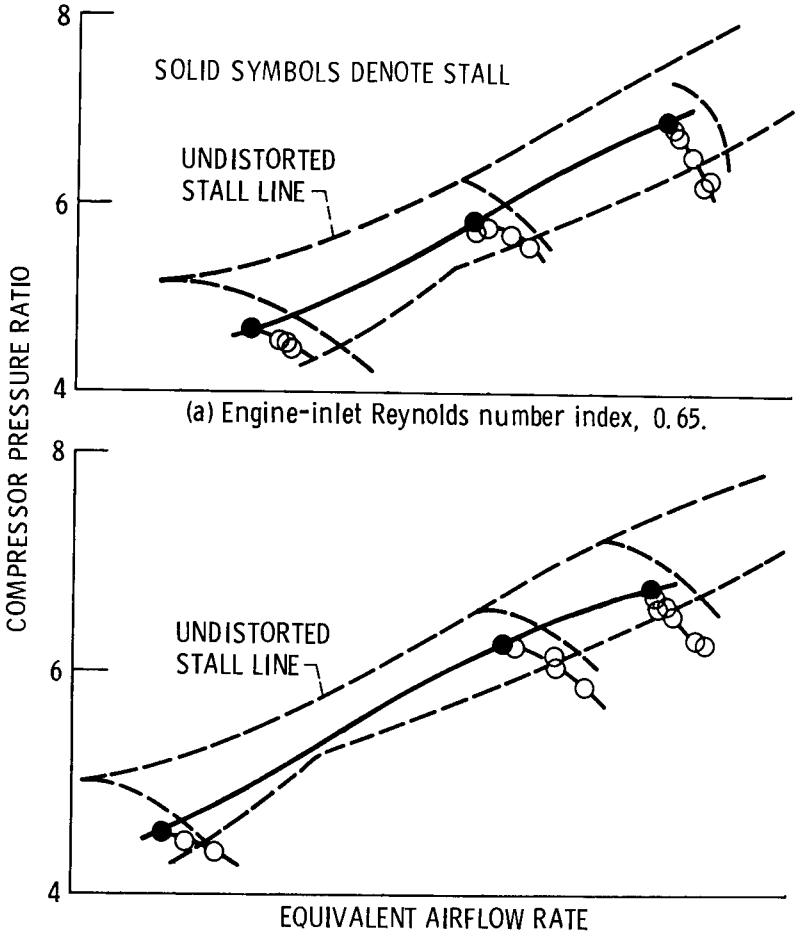

(a) Engine-inlet Reynolds number index, 0.65.

(b) Engine-inlet Reynolds number index, 0.30.

Figure 15. - Compressor performance with 180^0 extent circumferential distortion.

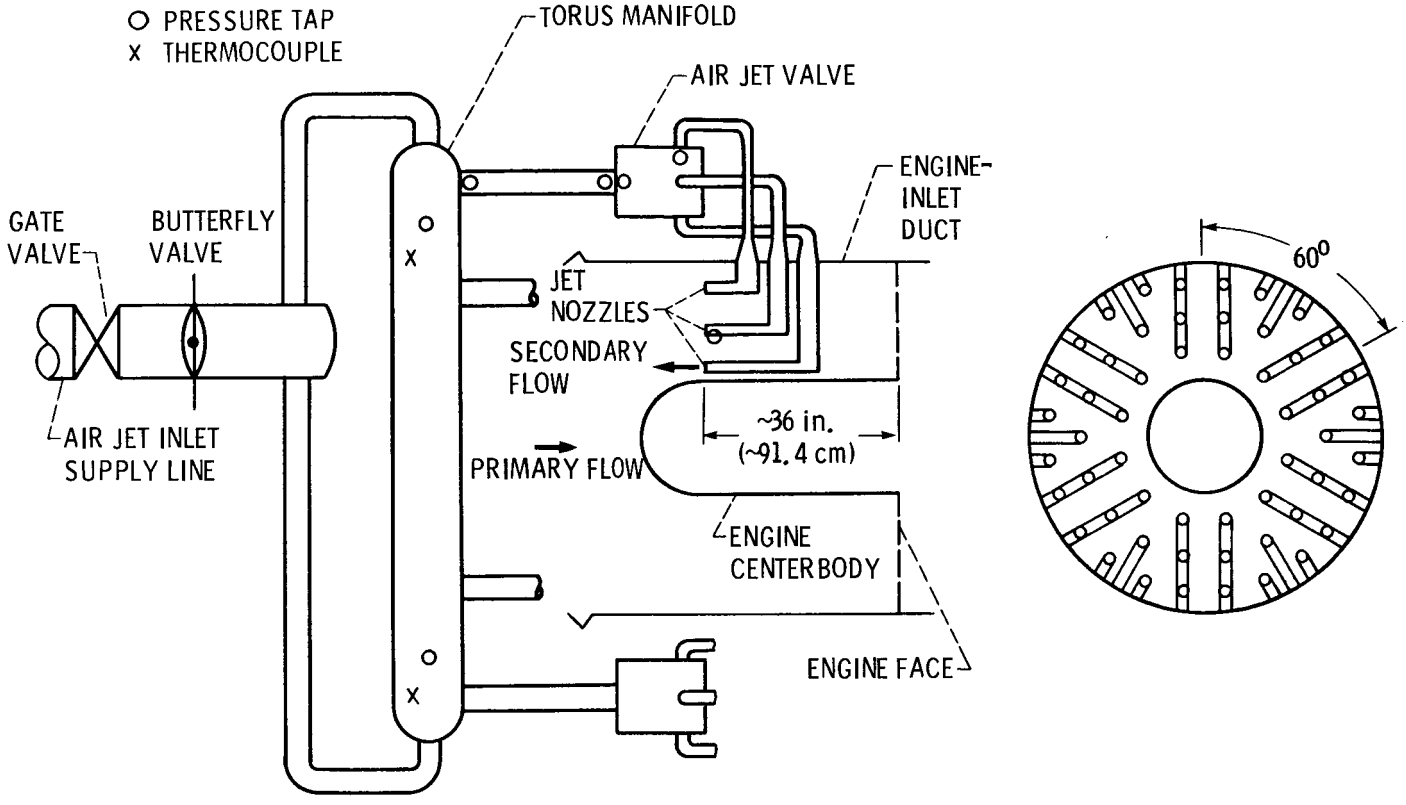

(a) Overall schematic.

(b) Frontal schematic of jets in engine-inlet duct.

Figure 16. - Air jet system.

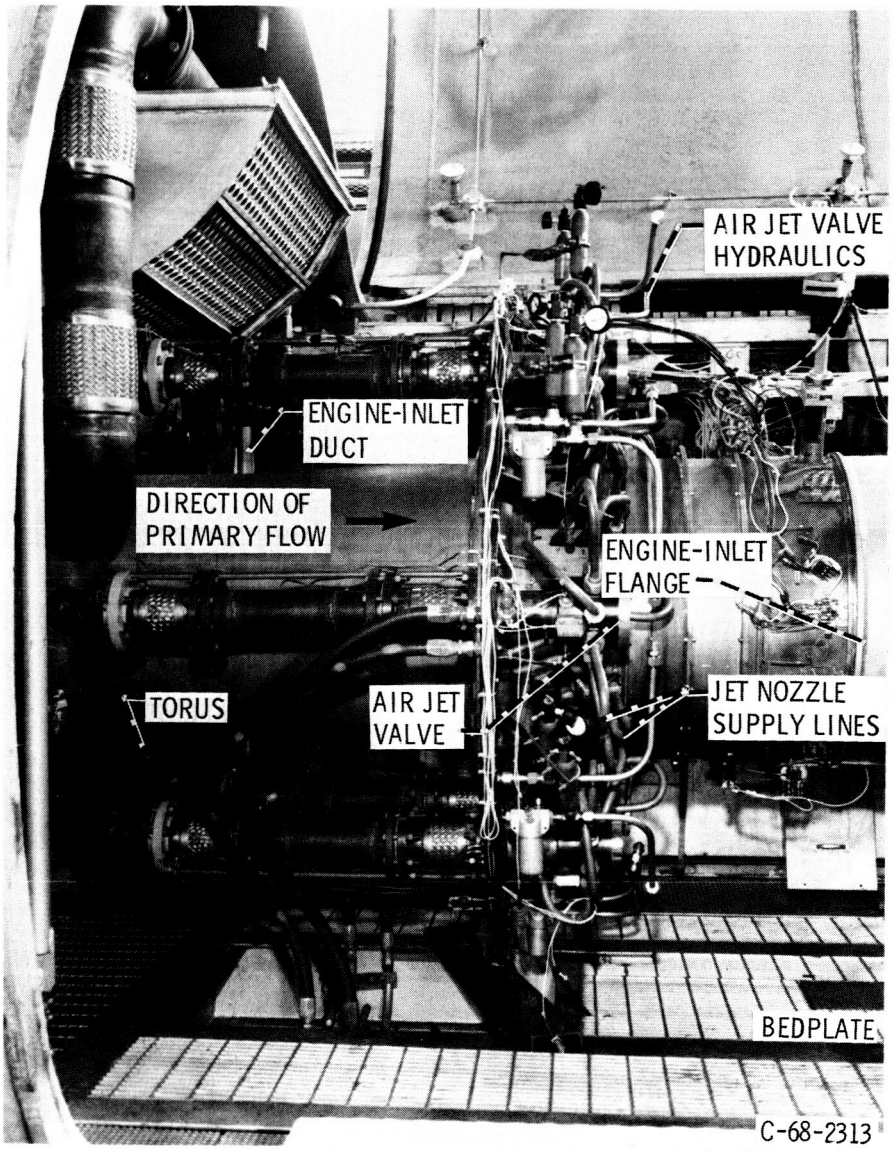

(c) Air jet system and engine-inlet duct.

Figure 16. - Continued.

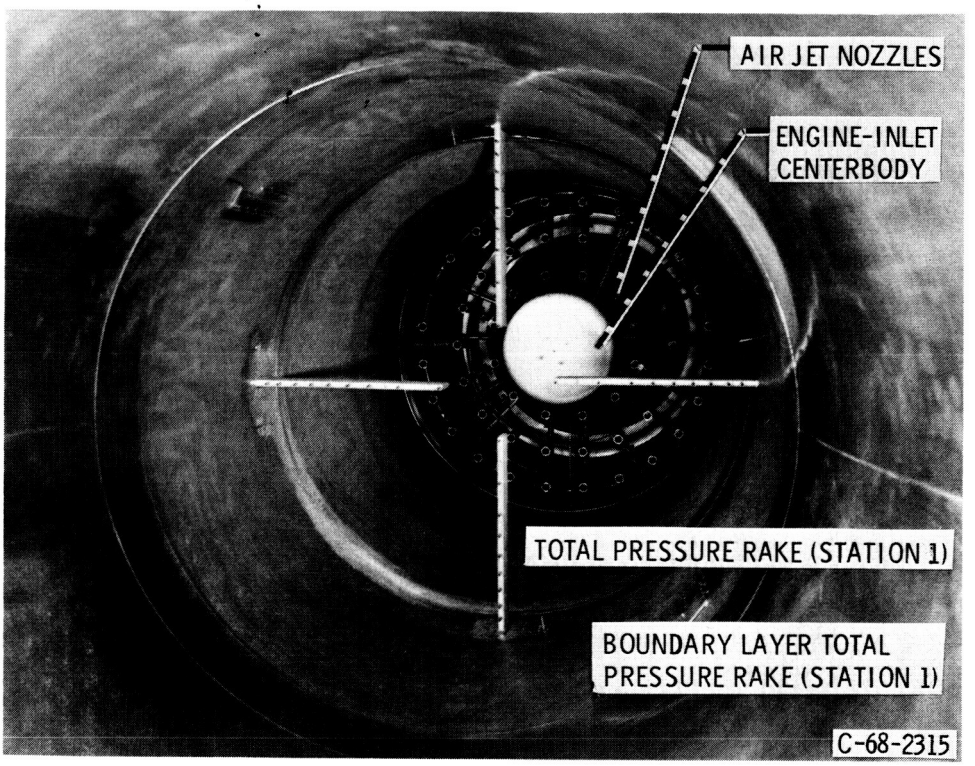

(d) Air jets installed in engine-inlet duct (view looking downstream).

Figure 16. - Concluded.

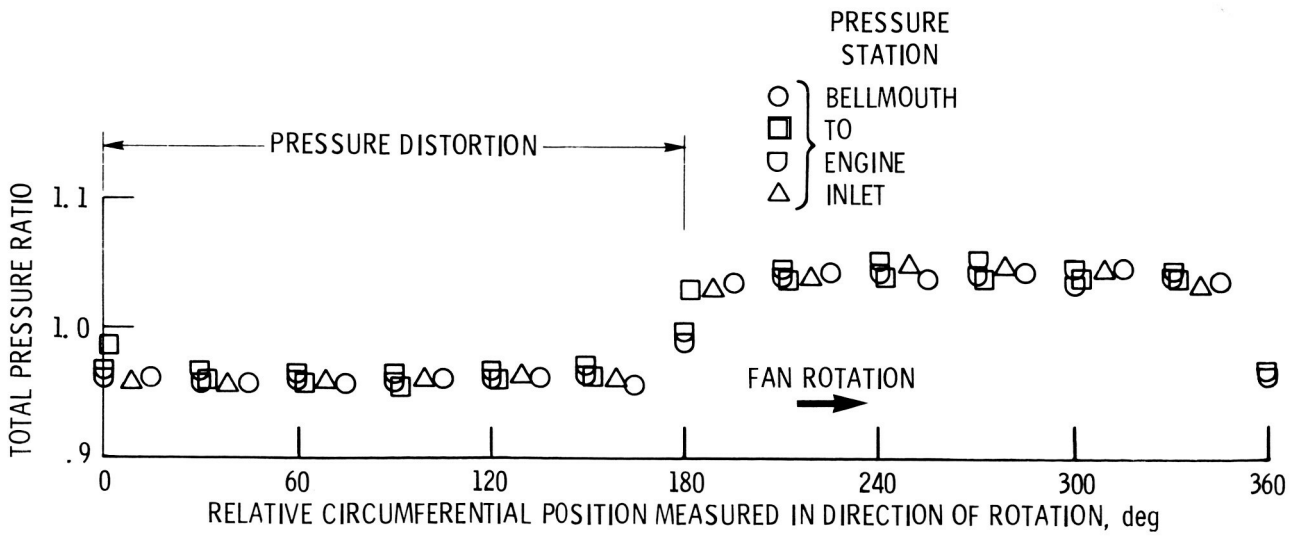

Figure 17. - Circumferential variation of total pressure profiles.

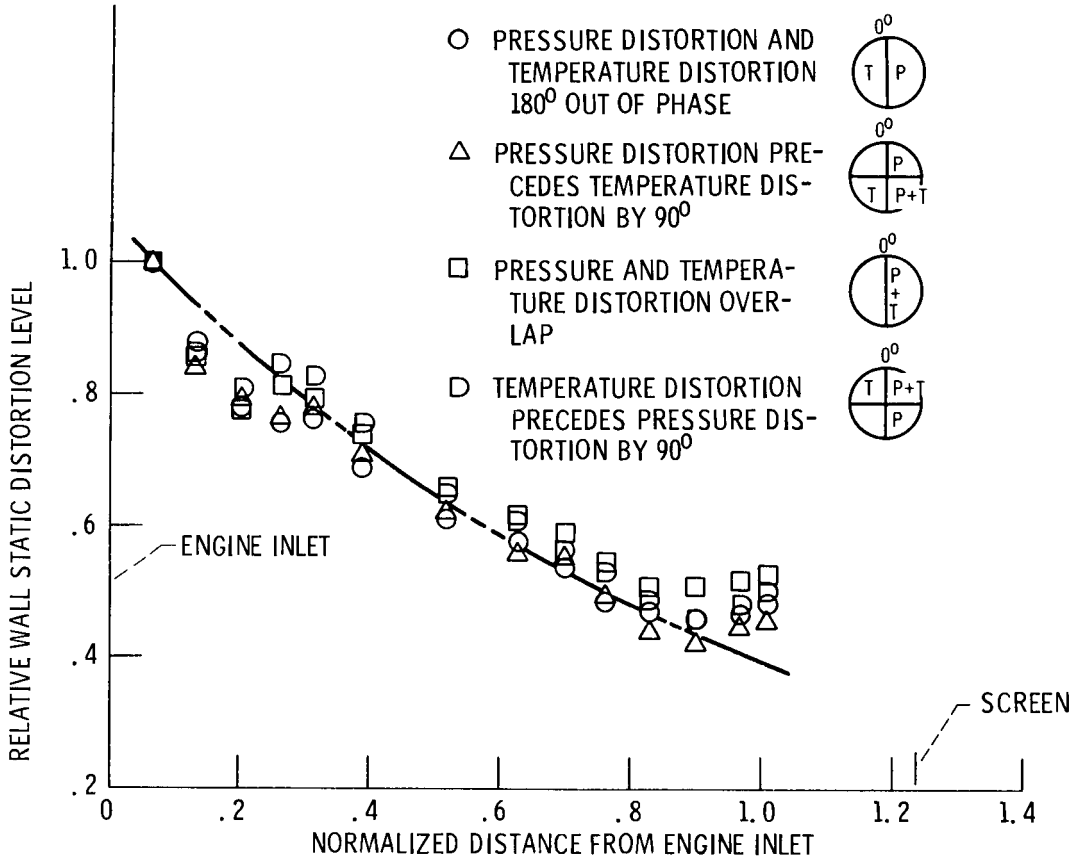

Figure 18. - Effect of total pressure and total temperature distortion orientation on static pressure distortion along inlet-duct wall.

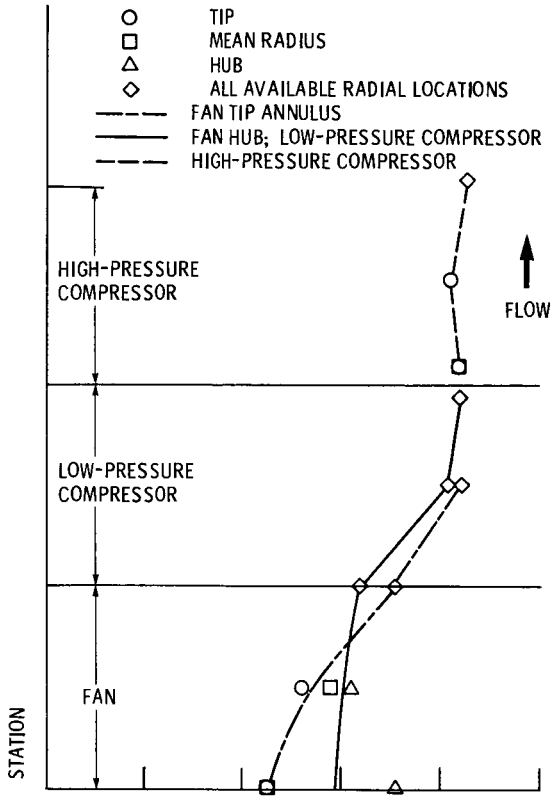

(a) Nominal low-speed-rotor speed, 7400 rpm.

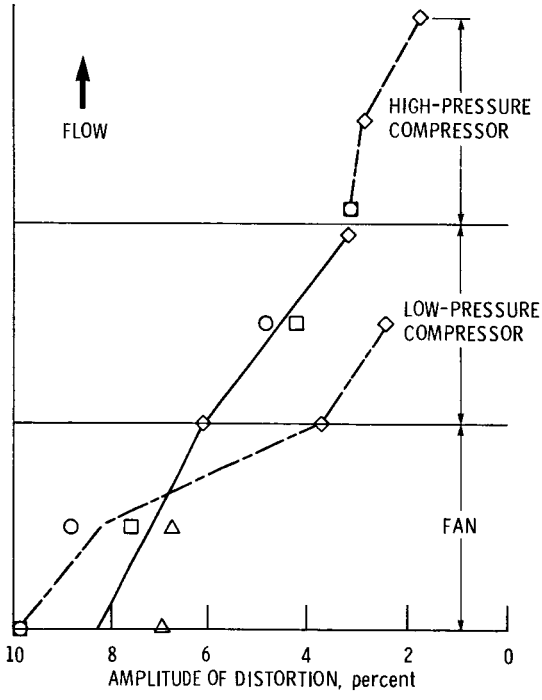

(b) Nominal low-speed-rotor speed, 8600 rpm.

Figure 19. - Total pressure distortion - axial variation in amplitude.

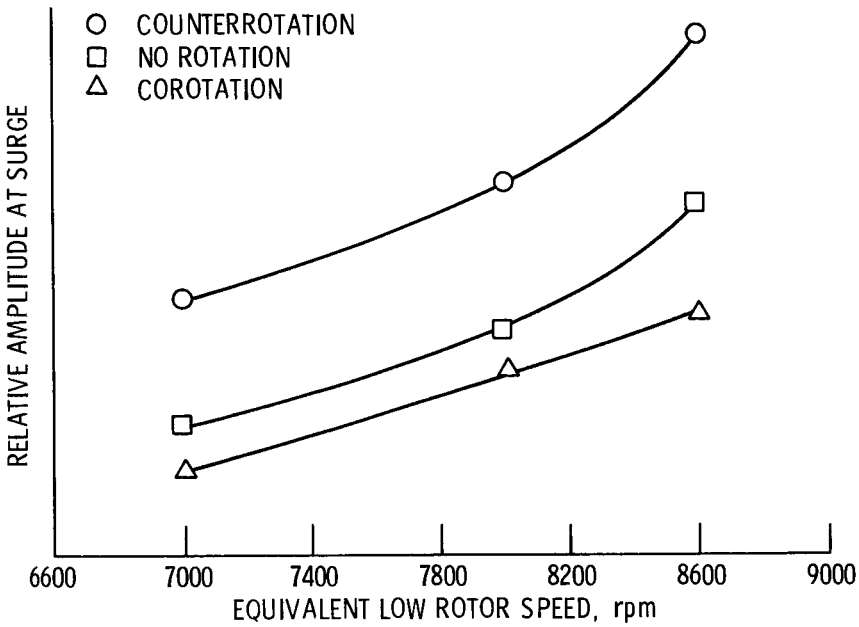

Figure 20. - Effect on stability of turbofan engine of rotating 180° square wave total pressure distortion at 20 Hz.

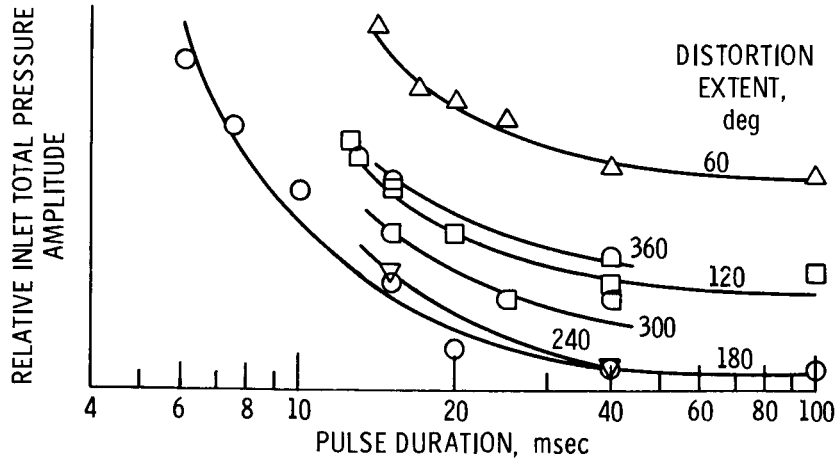

Figure 21. - Stall boundary as function of pulse amplitude, pulse duration, and distortion extent.

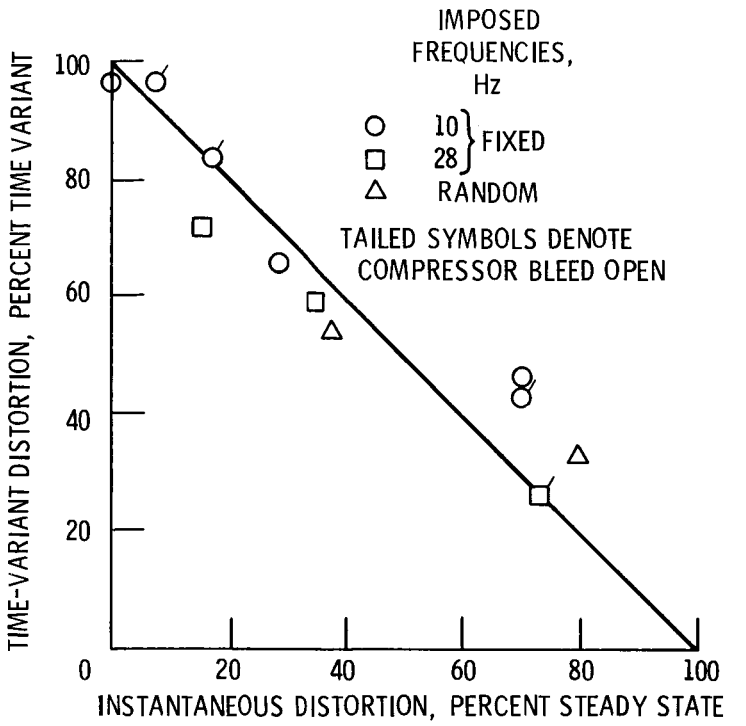

Figure 22. - Relation between steady-state and time-variant components of inlet flow distortion.

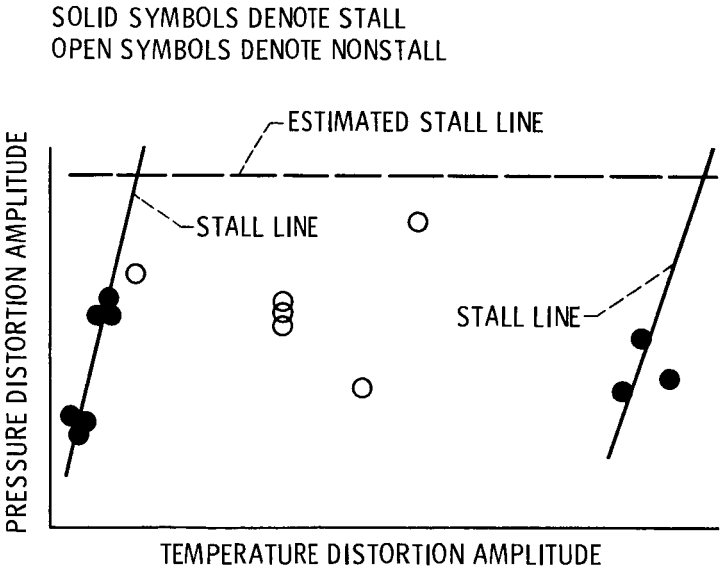

Figure 23. - Distortion sensitivity at engine inlet.

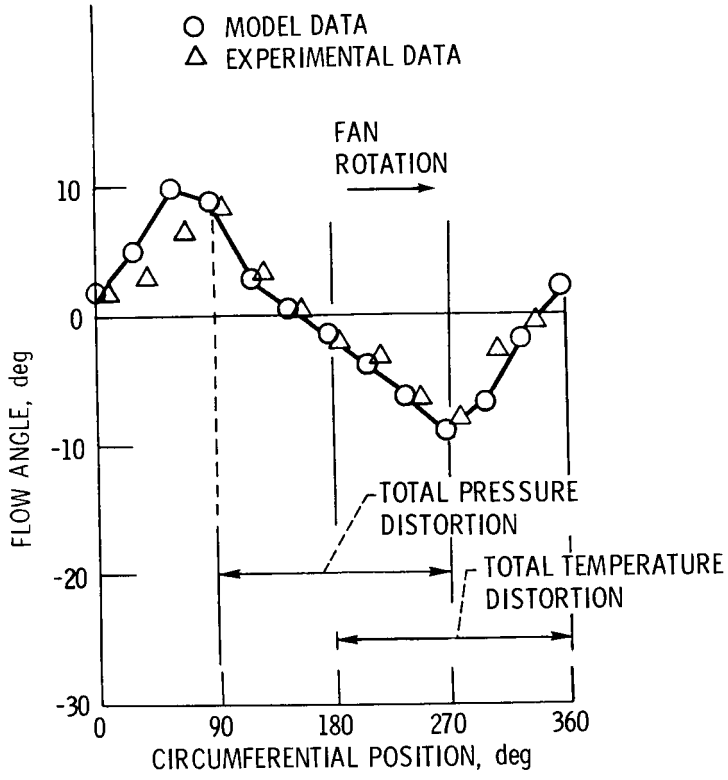

Figure 24. - Comparison of model and experimental approach angles for a complex flow distortion.

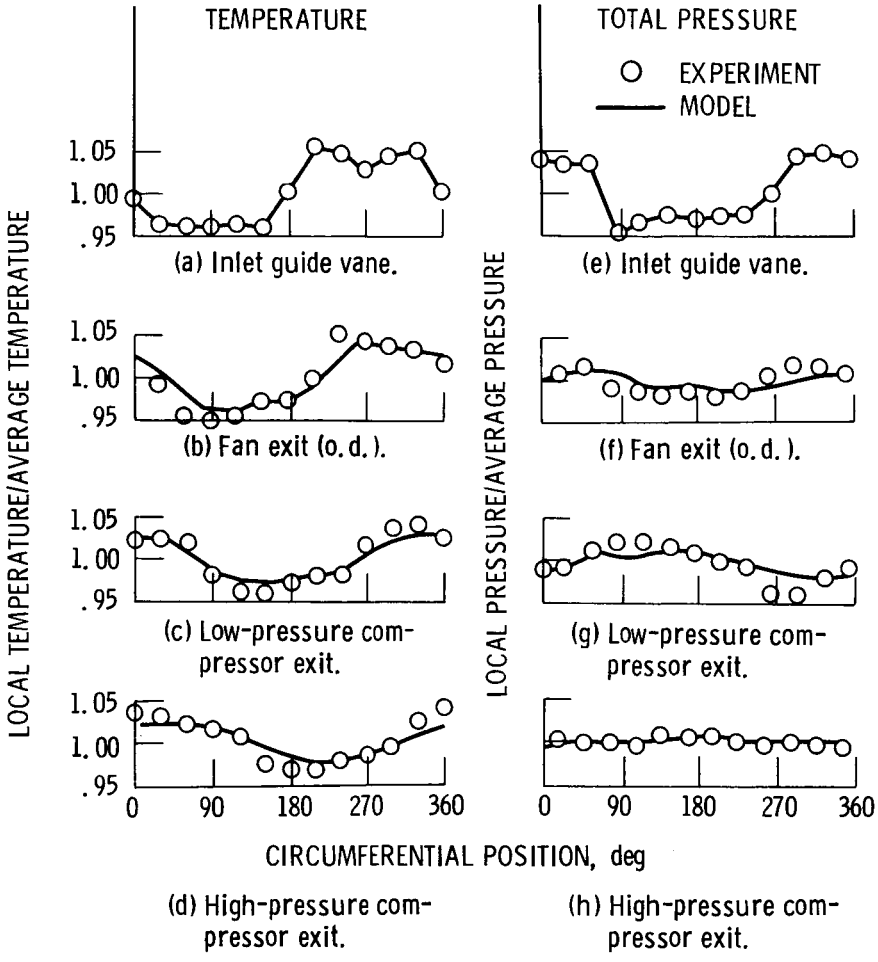

Figure 25. - Comparison of measured and predicted internal compressor profiles for combined pressure and temperature distortions.

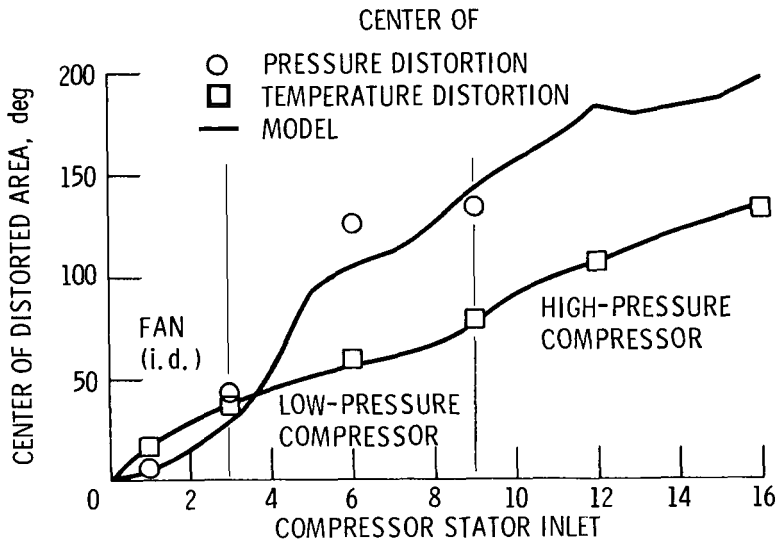

Figure 26. - Predicted swirl of total pressure and temperature distorted flow passing through compressor system.

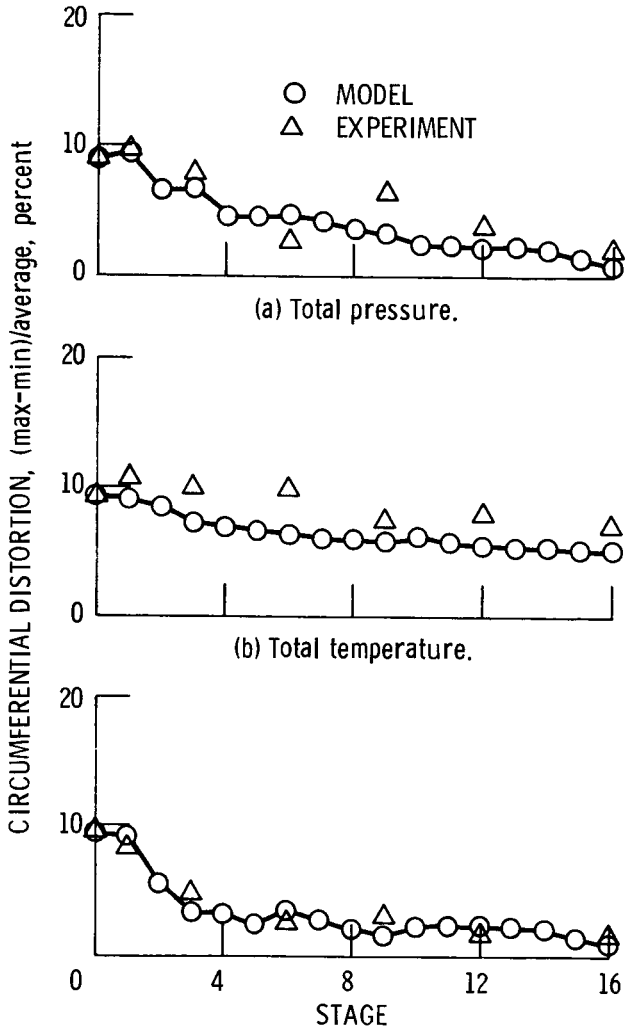

Figure 27. - Attenuation of distortion by compression system for combined pressure and temperature inlet distortion.

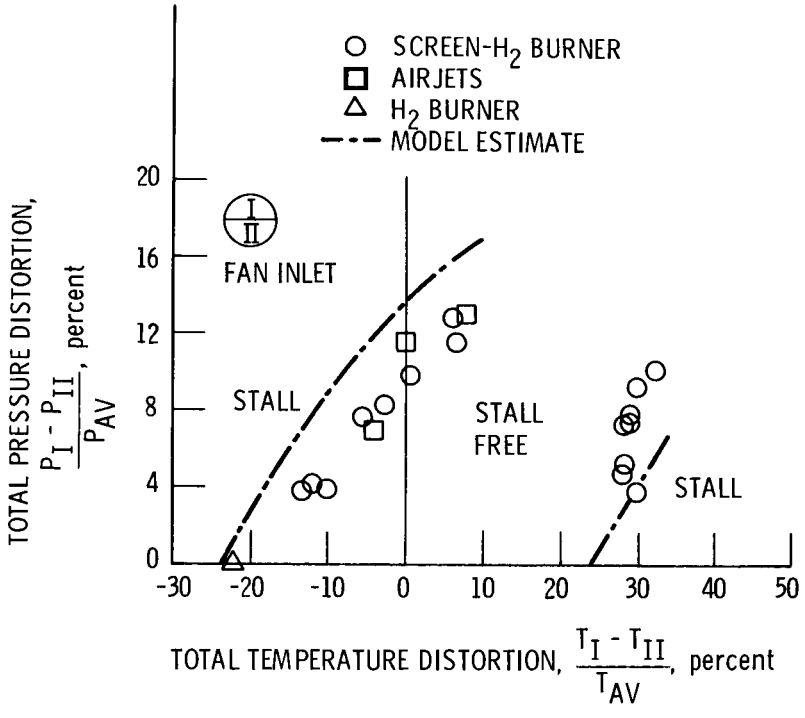

Figure 28. - Effect of relative position on limiting distortion for combined pressure and temperature distortions.

1. Report No.	2. Government Accession No.	3. Recipient's Catalog No.
NASA TM-87317		

4. Title and Subtitle	5. Report Date
Summary of Investigations of Engine Response to Distorted Inlet Conditions	
	6. Performing Organization Code: 505-68-51

7. Author(s)	8. Performing Organization Report No.
Thomas J. Biesiadny, Willis M. Braithwaite, Ronald H. Soeder, and Mahmood Abdelwahab	E-3048
	10. Work Unit No.

9. Performing Organization Name and Address	11. Contract or Grant No.
National Aeronautics and Space Administration Lewis Research Center Cleveland, Ohio 44135	
	13. Type of Report and Period Covered: Technical Memorandum

12. Sponsoring Agency Name and Address	14. Sponsoring Agency Code
National Aeronautics and Space Administration Washington, D.C. 20546	

15. Supplementary Notes

Prepared for the 68th Meeting of the Propulsion and Energetics Panel, sponsored by AGARD, Munich, Germany, September 8-9, 1986.

16. Abstract

A survey is presented of experimental and analytical experience of the NASA Lewis Research Center in engine response to inlet temperature and pressure distortions. This includes a description of the hardware and techniques employed, and a summary of the highlights of experimental investigations and analytical modeling. Distortion devices successfully simulated inlet distortion, and knowledge was gained about compression system response to different types of distortion. A list of NASA research references is included.

17. Key Words (Suggested by Author(s))	18. Distribution Statement
Engine tests; Inlet temperature; Inlet combined distortion; Distortion; Surge	Unclassified - unlimited STAR Category 07

19. Security Classif. (of this report)	20. Security Classif. (of this page)	21. No. of pages	22. Price*
Unclassified	Unclassified		

*For sale by the National Technical Information Service, Springfield, Virginia 22161